BIOCHEMICAL CHARACTERIZATION OF THE [FEFE]-HYDROGENASE MATURATION PROTEIN HYDE AND IDENTIFICATION OF THE SUBSTRATE

by

Nicholas William Bradford Boswell

A thesis submitted in partial fulfillment
of the requirements for the degree

of

Master of Science

in

Biochemistry

MONTANA STATE UNIVERSITY
Bozeman, Montana

August 2011

APPROVAL

of a thesis submitted by

Nicholas William Bradford Boswell

This thesis has been read by each member of the thesis committee and has been found to be satisfactory regarding content, English usage, format, citation, bibliographic style, and consistency and is ready for submission to The Graduate School.

Dr. Joan Broderick

Approved for the Department of Chemistry and Biochemistry

Dr. Bern Kohler

Approved for The Graduate School

Dr. Carl A. Fox

STATEMENT OF PERMISSION TO USE

In presenting this thesis in partial fulfillment of the requirements for a master's degree at Montana State University, I agree that the Library shall make it available to borrowers under rules of the Library.

If I have indicated my intention to copyright this thesis by including a copyright notice page, copying is allowable only for scholarly purposes, consistent with "fair use" as prescribed in the U.S. Copyright Law. Requests for permission for extended quotation from or reproduction of this thesis in whole or in parts may be granted only by the copyright holder.

Nicholas William Bradford Boswell

August 2011

ACKNOWLEDGEMENTS

First and foremost, I would like to thank Dr. Eric Shepard, without whom I would not be as advanced in my knowledge and skill of this project and bioinorganic chemistry in general as I am today. His assistance, guidance, and friendship have proved invaluable the past two years. He is the most valuable person to the Broderick lab and the Hydrogenase project, and in general is a really good guy (despite the fact he is a Penguins fan).

I would also like to thank Dr. Joan Broderick, Dr. John Peters, Dr. Robert Szilagyi, Dr. Trevor Rainey, and Dr. Bern Kohler for their assistance and guidance as my committee during my time here. Many thanks also go to rest of the Broderick group: Kaitlin Duschene, Rachel Hutcheson, Shourjo Ghose, Adam Crain, Ben Duffus, Krista Shisler, Amanda Byer, Dr. Tilak Chandra, and Dr. Sunshine Silver for their assistance, teaching, friendship, and listening to me talk probably too many times. The members of the Peters lab also are appreciated for guidance and assistance. Thank you to Dr. Charles Yocum, my undergraduate advisor, for his teachings and for encouraging me to come to Montana State University to work with Dr. Broderick.

My work was supported by the NASA Astrobiology Institute, Montana State University, Astrobiology Biogeocatalysis Research Center (NNA08CN85A) and by the Department of Energy (DE-FG02-10ER16194).

Finally, I would like to thank the many friends I have had throughout the department and elsewhere for all the good times in lab and outside of lab.

Go Blue!

TABLE OF CONTENTS

LIST OF FIGURES

Figure Page

LIST OF FIGURES – CONTINUED

Figure Page

LIST OF SCHEMES

Scheme Page

ABSTRACT

Hydrogenases catalyze the reversible reduction of protons using complex metal clusters with unusual ligands. The catalytic center of the [FeFe]-hydrogenases is called the H-cluster, and is characterized by a [4Fe-4S] cluster connected via a cysteine thiolate to a 2Fe subcluster coordinated by carbon monoxide and cyanide ligands as well as a bridging dithiolate. Assembly of the H-cluster is carried out by three hydrogenase maturation proteins: HydE, HydF, and HydG. HydF is a GTPase and has been implicated to serve as a scaffold for assembly of the 2Fe subcluster of the H-cluster. HydE and HydG are radical S-adenosylmethionine (SAM) enzymes and thus are thought to utilize reductive cleavage of SAM to initiate radical chemistry. HydG has been shown to catalyze the formation of the carbon monoxide and cyanide ligands of the H-cluster utilizing tyrosine as a substrate. HydE, therefore, has been proposed to be responsible for biosynthesis of the dithiolate ligand of the H-cluster. The aim of this study was to biochemically characterize active, Fe-S reconstituted HydE and to identify the substrate of this radical SAM enzyme. Questions to be studied also included studying the role of HydE in H-cluster maturation. This study used protein purified from recombinant *E. coli*. The purified protein was chemically reconstituted with iron and sulfide, and used for spectroscopic characterization and HPLC based activity assays. Colorimetric assays were also used for protein characterization and to test for the consumption of substrate. The results indicate that cysteine is likely the substrate of HydE. Activity assays show that HydE- catalyzed SAM cleavage is stimulated in the presence of cysteine, and HydF purified from different genetic backgrounds shows a spectroscopic shift in the λ_{max} when both HydE and cysteine are present during growth. Spectroscopic characterization confirms that HydE is an Fe-S containing radical SAM enzyme and that cysteine may be a substrate during [FeFe]-hydrogenase H-cluster maturation.

INTRODUCTION

Interest in hydrogenases has grown dramatically over recent years primarily because of its implication as a new source or model for a renewable fuel source. The ability of the enzymes to produce H_2 from abundantly occurring protons and electrons creates excitement for the ability to create biomimetic models of these enzymes and possibly use them for biological H_2 harvesting for renewable resource alternatives to fossil fuels. Many synthetic clusters have been developed so far that attempt to mimic the organometallic clusters of hydrogenases, but these mimics have not been able to recreate the efficiency of [FeFe]-hydrogenase. Characterization of the biochemical pathway of H-cluster synthesis is crucial to fully understand the biochemistry of hydrogen metabolism and should aid in the ability to recreate the clusters for non-biological use.

Iron-Sulfur Clusters

Iron-sulfur (Fe-S) clusters have been found to be prevalent in all of biology and participate in many necessary biological functions such as electron transfer, metabolism, iron regulation, cofactor biosynthesis, regulation of gene expression, and protein stability. This omnipresence in biology and biological functions suggests that Fe-S clusters are very ancient in origin (*1*). Fe-S clusters come in many different forms, the most common of which are the [2Fe-2S] rhomb or the [4Fe-4S] cubane. There are other types though such as a [3Fe-4S], which is similar to the cubane structure but lacking one of the irons. Beyond simple clusters such as these, there are also complex Fe-S clusters such as those

found in enzymes like carbon monoxide dehydrogenase, nitrogenase, and hydrogenase (*2*). Non-complex Fe-S clusters are biologically synthesized by proteins encoded by the sulfur mobilization *(suf)*, nitrogen fixation *(nif)*, and Fe-S cluster *(isc)* operons (*3-5*). The protein systems encoded by these operons all operate in a similar manner, utilizing a cysteine desulfurase as a sulfide source, another protein to act as a scaffold, and other proteins to assist in Fe-S cluster biosynthesis (*6, 7*). In the Isc protein machinery IscU acts as a scaffold for the Fe-S cluster assembly, the key to which is an invariant aspartate residue that aids in cluster transfer to apoprotein targets (*8-10*). IscU receives sulfur from a cysteine desulfurase IscS, implicating cysteine is the source of sulfide in Fe-S clusters(*4, 11*). The source of iron has not yet been fully resolved and there is not yet a unifying concept for iron transfer, but experimental evidence suggests IscA, an A-type protein (*12-15*), or the iron storage ferritin proteins (*16-18*) as possible iron sources.

Hydrogenases

The hydrogenase with the simplest metal cofactor, [Fe]-hydrogenase, has an active site that consists of a single Fe atom ligated by two CO ligands, a cysteine side chain, a guanylyl pyridinol cofactor, and an unknown ligand that is possibly an acyl group (*19*). Another name for [Fe]-hydrogenase is H_2-forming methylenetetrahydromethanopterin (H_4MPT) dehydrogenase (Hmd), and as the name indicates, the enzyme reversibly catalyzes the dehydrogenation of methylene-H_4MPT. The reason this enzyme is included among the hydrogenases is that H_2 is produced as a by-product of its reaction. [NiFe]-hydrogenases contain a heteronuclear cluster of a Ni

atom linked to an Fe atom by two bridging cysteine thiolates and another linker of which the identity is unknown. The Ni is additionally ligated by two other cysteine thiolates, while the Fe atom is decorated with two cyanide ligands and one carbonyl moiety (*20*). Along with [FeFe]-hydrogenase, [NiFe]-hydrogenase is considered a "true" hydrogenase, in that its catalyzed reaction is the reversible reduction of protons to H_2 (Eq. 1):

$$H_2 \leftrightarrow 2H^+ + 2e^- \text{ (Eq. 1)}$$

The maturation of the heterometallic cluster in [NiFe]-hydrogenase has been extensively studied, and it has been shown that at least seven accessory proteins are required. HypE and HypF supply the cyanide ligands from a carbamoyl phosphate source. HypF adenylates carbamoyl phosphate and transfers it to a COOH-terminal cysteine on HypE where it is dehydrated and forms a thiocyanate ligand to the cysteine (*21*). Delivery of these ligands is accomplished by a HypD/HypC complex. HypB and HypA work together to insert the Ni atom into the cluster. Currently, the source of the CO ligand is unknown, but it is known that carbamoyl phosphate is not the source so the biosynthesis of the CO ligand follows a different route than the CN^- ligands (*22*). Much less is known about the maturation process of [Fe]-hydrogenase, but recent work has discovered two genes flanking the gene encoding the [Fe]-hydrogenase (*hmdA*). These genes, *hmdB* and *hmdC*, are putative maturation proteins for this hydrogenase. HmdB has been identified as a radical-SAM protein while *hmdC* shows sequence homology to an eukaryotic fibrillarin. Some preliminary characterization has been done on these enzymes, but the maturation process of [Fe]-hydrogenase is still unresolved (*23*).

The active site of [FeFe]-hydrogenase, the H-cluster, is composed of a [4Fe-4S] cubane attached by a cysteine thiolate to a 2Fe subcluster with CO and CN^- ligands and a dithiolate linker (Figure 1.1) (*24-26*). Besides the H-cluster, [FeFe]-hydrogenase from *Clostridium pasteurianum* (CpI) contains four additional Fe-S clusters, three of which are [4Fe-4S], and the other being a [2Fe-2S] cluster. These clusters are assumed to aid in electron transfer between the protein surface and the active site. As seen in Figure 1.2, the distance between all the clusters, with the exception of the distance between the two clusters on the surface, is less than 11 Å, which is reasonable for electron transfer in proteins since there may be aromatic residues in those areas to aid in electron shuttling. Additionally, there is a basic patch on the protein surface associated with the [4Fe-4S] closest to the surface and an acidic domain on the protein surface associated with the [2Fe-2S] cluster, which gives the hydrogenase the ability to interact with a variety of electron donors and acceptors, likely to be ferredoxin proteins (*27*). Structural evidence suggests that the catalytic reaction takes place on the terminal Fe site of the 2Fe subcluster of the H-cluster. A water molecule has been observed to be ligated to the distal Fe in the CpI structure but not on the *Desulfovibrio desulfuricans*. A water molecule is bound to one hydrogenase structure but not the other due to the fact that the H-cluster in the CpI structure was likely in an oxidized or resting state, while the active site in the *D. desulfuricans* is likely in a more reduced or turnover state. As a non-substrate ligand, the water is in prime position for displacement by the substrate (H^+) and formation of a bound hydride intermediate (*28*). The hypothesis that catalysis occurs on the terminal Fe of the 2Fe subcluster is further supported by a crystal structure with

exogenous CO bound to the terminal Fe in place of water yielding inactive enzyme (Fig. 1.1). The bound CO saturates the coordination sites with strong ligands and thus inhibits catalysis (*29*).

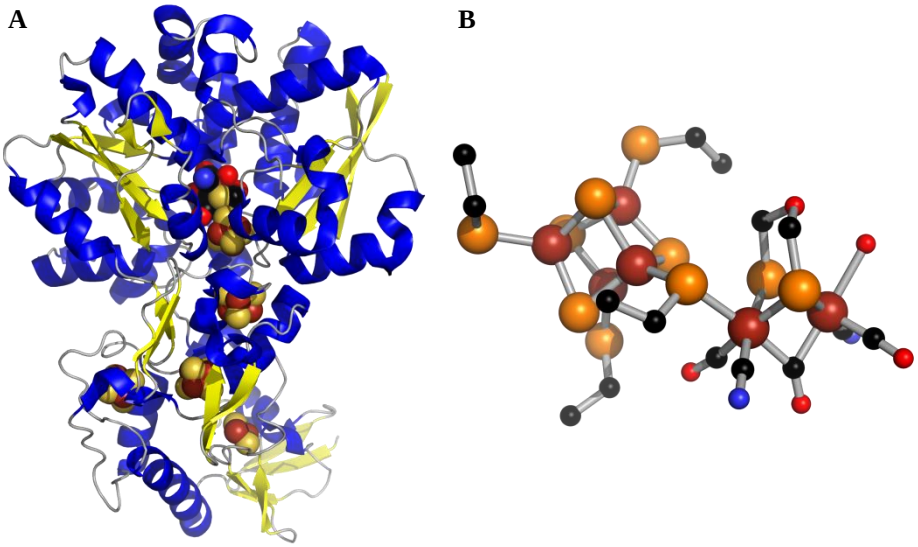

Figure 1.1 (A) Ribbon representation of *Clostridium pasteurianum* (CpI) [FeFe]-hydrogenase (PDB code: 3C8Y) (B) Close-up of the H-cluster shown in ball and stick form.

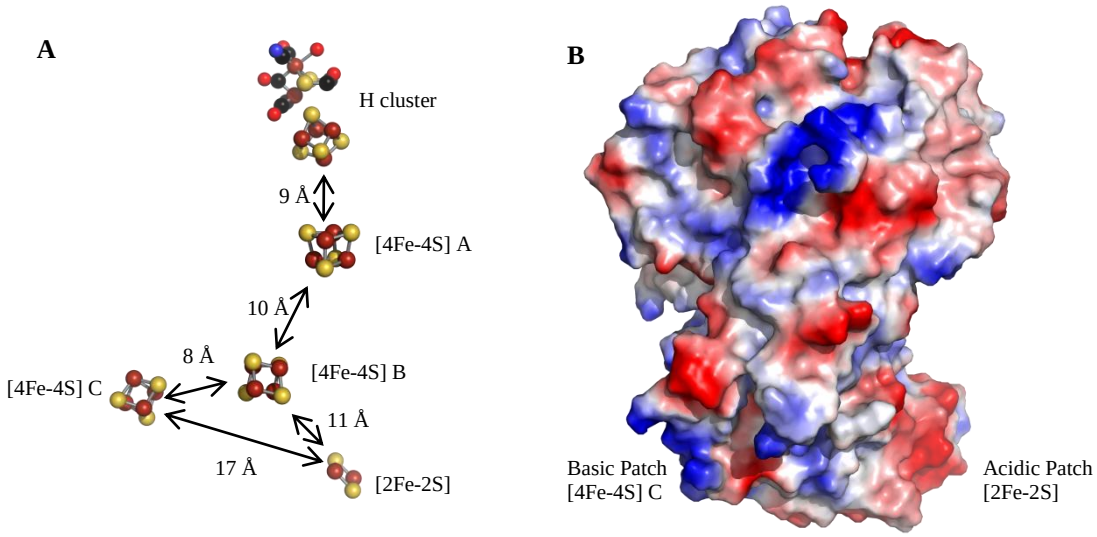

Figure 1.2. (A) Fe-S clusters of CpI [FeFe]-hydrogenase, highlighting the inter cluster distances. (B) Relative surface charge of [FeFe]-hydrogenase, with areas of acidic residues colored red and areas of basic residues colored blue. Adapted from ref. 27.

To explore necessary genes for active [FeFe]-hydrogenase, random insertional mutants in *Chlamydomonas reinhardtii* were screened for the inability to produce H_2. The study revealed that two genes produced proteins necessary for [FeFe]-hydrogenase activation, *hydEF* and *hydG* (in eukaryotes, the *hydE* and *hydF* genes are fused, but they exist as separate genes in prokaryotes) (*30, 31*). These three gene products have been shown to be sufficient for [FeFe]-hydrogenase activation. [FeFe]-hydrogenase from *C. reinhardtii* expressed in the absence of maturation proteins ($HydA^{\Delta EFG}$) has been shown to contain a requisite [4Fe-4S] cluster, upon which the 2Fe subcluster of the H-cluster is attached (*32*), indicating the maturation proteins are only responsible for the formation of the two iron subunit. The maturase proteins HydE and HydG have been identified as radical S-adenosylmethionine (SAM) enzymes, and HydF has been shown to be a GTPase (*30, 31*).

Radical SAM Enzymes

The radical SAM superfamily comprises more than 2800 proteins, most of which contain the canonical amino acid sequence motif CxxxCxxC, which binds a [4Fe-4S] cluster (*33, 34*). As seen in Fig. 1.3, the cluster is coordinated by three cysteines with one "unique" iron that is not ligated to the protein. This unique iron is the binding site of SAM, which is reductively cleaved to form a 5'-deoxyadenosyl (dAdo) radical intermediate (Figure 1.4) (*35-47*). The dAdo radical abstracts a hydrogen atom from a substrate that is then involved in one of the diverse chemical reactions characterized by this enzyme superfamily such as sulfur insertion, generation of protein based glycyl radicals, heme biosynthesis, and DNA repair. The deoxyadenosyl radical is formed when SAM binds the unique iron site via its amino and carboxyl groups and one electron is transferred to SAM from the cluster via an inner sphere mechanism to the sulfonium ion of SAM (*35-37, 39*). In most radical SAM enzymes characterized so far, SAM acts a cosubstrate and is converted to methionine and 5'-deoxyadensosine. In cases such as lysine 2,3-aminomutase (LAM) (*48-50*) and spore photoproduct lyase (SPL) (*51-53*), SAM is used as a cofactor where the product radical reabstracts a hydrogen from 5'-deoxyadenosine to reform the 5'-deoxyadensosyl radical. This then reacts with methionine to reform SAM and the reduced cluster on the enzyme (*34*). The radical SAM enzymes structurally characterized to date contain either a partial or complete triose phosphate isomerase (TIM) barrel. Enzymes such as biotin synthase (BioB) and HydE have complete $(\beta/\alpha)_8$ TIM barrels, while smaller enzymes such as pyruvate-formate lyase activating enzyme (PFL-AE) have an incomplete $(\beta/\alpha)_6$ TIM barrel. The size of the TIM

barrel is suggested to be related to the size of the substrate, as an incomplete TIM barrel as in PFL-AE can accommodate a protein substrate, while the full TIM barrel in HydE and BioB can likely only accommodate a small molecule substrate (*54*). The [FeFe]-hydrogenase maturation proteins HydE and HydG are not the only enzyme examples for which radical SAM chemistry is involved in metallocofactor biosynthesis. Another example is the nitrogenase maturation enzyme NifB, which is involved in the assembly of the FeMo-co cluster in nitrogenase. A final example is the newly discovered protein HmdB which is suggested to be involved in the development of the [Fe]-hydrogenase active site (*23, 55*). Curiously, HydE, HydG, and HmdB are clustered in a well-supported sequence lineage, indicating they all recently diverged from a common ancestor and may catalyze similar reactions (*56*).

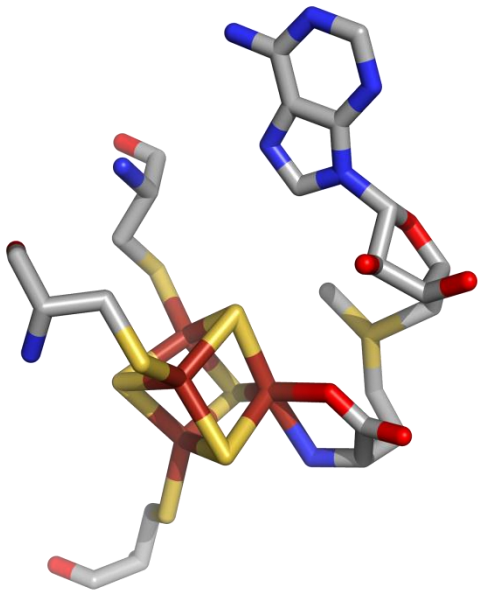

Figure 1.3. Structural view of SAM binding to the [4Fe-4S] cluster of pyruvate formate-lyase activating enzyme. Adapted from ref. 47.

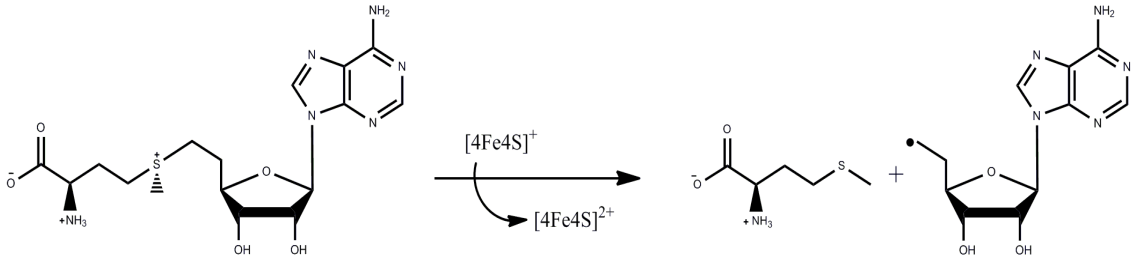

Figure 1.4. Mechanism of cleavage of S-adenosylmethionine by a $[4Fe\text{-}4S]^{+}$ cluster, forming methionine and a 5'-deoxyadenosyl radical. Adapted from ref. 34.

[FeFe]-Hydrogenase Maturation

HydF and HydG

The exact mechanism of H-cluster biosynthesis is still mostly unknown, but recent reports have provided insight into the possible roles of each of the maturation proteins and a theoretical mechanism of cluster assembly. HydF has been demonstrated to be the assembly scaffold of the 2-Fe subcluster of the H-cluster (*57*). The EPR spectrum of HydF expressed in the absence of HydE and HydG ($HydF^{\Delta EG}$) exhibits a signal indicative of a $[2Fe\text{-}2S]^{+}$ cluster in the enzyme. When HydF is expressed in a background of HydE and HydG ($HydF^{EG}$), the paramagnetic $[2Fe\text{-}2S]^{1+}$ cluster signal is lost, which is consistent with HydE and HydG modifying the cluster to an EPR silent H-cluster precursor (*57*). Moreover, FTIR spectroscopy demonstrated the presence of a CO and CN^{-} ligated iron species on $HydF^{EG}$ providing additional support for the hypothesis that HydE and HydG modify a [2Fe-2S] precursor cluster on HydF to the 2Fe subcluster of the H-cluster (*57*).

Radical SAM enzymes have been observed to reductively cleave SAM in the absence of substrate, which is termed non-productive cleavage (*53, 58-68*). A

characteristic of radical SAM catalysis is that rates of non-productive SAM cleavage are relatively slow in the absence of substrate molecules; addition of substrate can significantly increase the rates of SAM cleavage and dAdo production (*53, 62, 69, 70*). The substrate for HydG was recently discovered by screening potential small molecule substrates for enhanced levels of dAdo production (*70*). Accordingly, tyrosine was discovered to stimulate dAdo production by a factor of five, and *p*-cresol was identified as one of the turnover products (*70*). The other putative reaction product from the HydG reaction was proposed to be a dehydroglycine intermediate, although a recent report has suggested it is a glycyl radical (*71*). Regardless of the exact chemical composition of the intermediate species, CO and CN^- have both been shown to be derived from the HydG catalyzed degradation of tyrosine (*72, 73*). This is the first instance for any hydrogenase that enzyme catalyzed CO synthesis has been demonstrated despite all that is known about maturation of [NiFe]-hydrogenase (*72, 73*).

HydE

With HydF acting as a scaffold and HydG producing CO and CN^-, the process of elimination would indicate that HydE is responsible for synthesis of the dithiolate bridging ligand. This bridging ligand has been proposed to be dithiopropane, dithiomethylamine, or dithiomethylether. HYSCORE spectroscopy studies combined with DFT calculations have shown that dithiomethylamine is the most likely bridging ligand. A nitrogen atom, as opposed to a carbon in dithiopropane, as the central atom of the bridging dithiolate could act as a base, accepting a proton during molecular hydrogen splitting (*74*). The substrate, as of yet, is still under investigation, but it is likely a small

common metabolite present in *E. coli*, as hydrogenase activation has been demonstrated in systems overexpressing HydE, HydF, and HydG in *E. coli*. In an experiment using purified HydA and whole cell extracts of the maturase enzymes it has been shown that hydrogenase activity is stimulated by the addition of tyrosine, cysteine, and SAM (Fig. 1.5) (*75*). The reason for SAM and tyrosine stimulation are attributed to radical SAM chemistry and the demonstration that tyrosine is the substrate for HydG (*70*). This result would suggest cysteine as a possible substrate for HydE, although cysteine alone was not able to stimulate hydrogenase activity, suggesting a synergistic effect between cysteine, tyrosine, SAM and a HydE and HydG protein complex may be functioning *in vivo*.

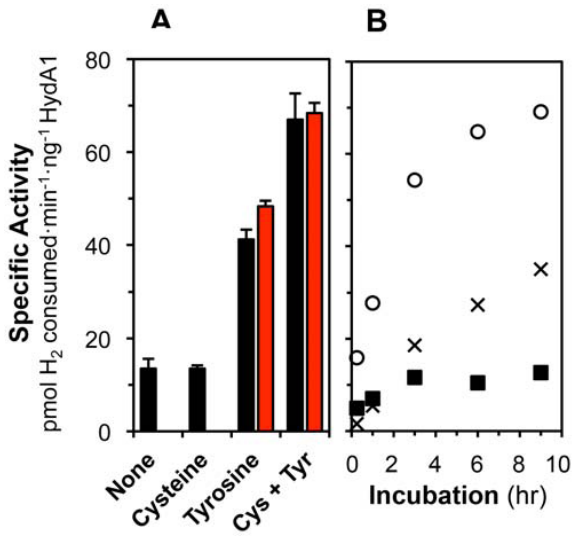

Figure 1.5. Effects of cysteine and tyrosine on HydA activity *in vitro*. Black bar represent as-isolated enzyme and red bars represents reconstituted HydA, and reconstituted protein was not tested for no additions and addition of cysteine only (left). Full squares represent addition of cysteine only, crosses represent addition of tyrosine only, open circles represent addition of both cysteine and tyrosine (right). Reprinted from reference 75.

Computational work has been useful in predicting potential identities of the dithiolate linker, though all three possibilities have been argued to be probable. Most

recently, DFT studies have looked into possible mechanisms for insertion of the dithiolate linker onto the 2Fe subcluster of the H-cluster. The study explored mechanisms in which dithiopropane, dithiomethylamine, and dithiomethylether would be formed. The study concluded that the so-called C-path (mechanism for dithiopropane formation) would be most likely, considering the absence of energetically high-lying intermediates, as opposed to the O- and N-paths. The C-path is also achievable in much fewer mechanistic steps than the other two. However, the authors of this study do not rule out the possibility of a more complex substrate that contains a methylaminoalkyl or methoxyalkyl chain that could create dithiolate ligands with the central atom being O or N (*76*). Furthermore, quantum refinement studies, combining the crystal structure coordinates with DFT calculations, and ^{57}Fe-ENDOR studies suggested again that dithiomethylamine is the most likely identity of the bridging dithiolate ligand (*77*, *78*). All of the methods described here to discern the identity of the bridge-head atom of the dithiolate ligand are indirect methods and will only be able to describe what the identity of the atom is most likely to be. At this point, the only way to be able to definitively characterize the full dithiolate ligand is to fully characterize the enzyme reaction of HydE.

Rubach *et al*. have characterized HydE from *Thermotoga maritima* and have demonstrated its ability to cleave SAM, confirming its identity as a radical SAM enzyme (*65*). In this study, the protein was aerobically purified, then reconstituted under anaerobic conditions. Reconstitution of the protein achieved a maximum of eight iron atoms per protein. The EPR results of this study show that the Fe-S cluster contained in

the enzyme is a [4Fe-4S] cluster. The authors demonstrated that the reconstituted HydE cleaved SAM at a rate of 1 mol dAdo/mol protein/hour. Several turnovers were achieved, indicating that the enzyme is catalytic in nature (*65*).

The X-ray crystal structure of HydE from *Thermotoga maritima* has been solved and can be seen in Figure 1.6. The structure shows that HydE has a distorted triose-phosphate isomerase (TIM)-barrel, which are commonly found in the structures of radical SAM enzymes. There is a lid loop at the top of the TIM-barrel, possibly acting as a gateway for substrate access to the active site. The putative active site is located near the top of the TIM-barrel, and the study yielded proposed substrate/product channels using a 1.0 Å probe. The possible location of the active site was based primarily on the location of the site-differentiated iron-sulfur cluster. The putative active site location was also demonstrated using molecular docking, where carboxylate moieties and partial positive charges on molecules commonly bound opposite each other surrounding a sphere where radical transfer should occur. The authors of the study also attempted to soak the crystals in common metabolites to get a possible structure with a putative substrate or product bound, but the only molecule that stuck was thiocyanate. Thiocyanate binding provided information regarding an anionic binding site near the proposed active site where radical chemistry would be performed, but nothing conclusive could be said regarding possible substrate or product molecules (*46*). In a more recent crystal structure solved to higher resolution from the same organism, it was found that methionine and 5'-deoxyadenosine both bind the protein very tightly and a structure was obtained with these molecules bound near the [4Fe-4S] cluster. This result could suggest that HydE uses SAM as a

cofactor rather than a cosubstrate (*79*). In the computational work described above, if the C-path was used, HydE would need to act as a bifunctional enzyme. This would provide a possible explanation for methionine and 5'deoxyadenosine binding so strongly to HydE and the fact that SAM turnover to 5'deoxyadenosine has been demonstrated experimentally (*76*).

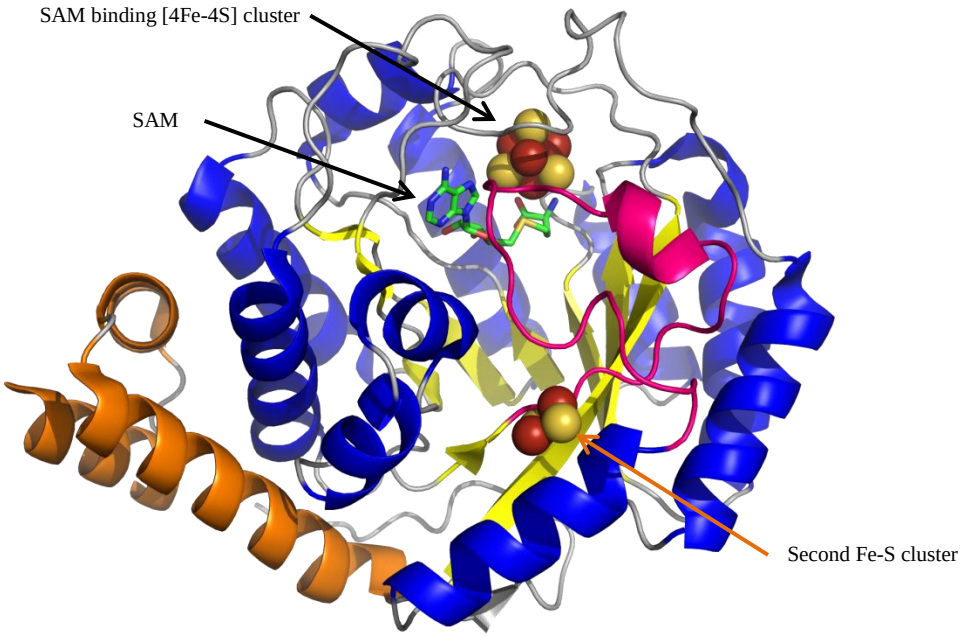

Figure 1.6. X-Ray crystal structure of HydE from *Thermatoga maritima*. TIM barrel is shown in yellow and blue, the lid loop is shown in pink.

The X-ray crystal structure of HydE also demonstrates the presence of a second [Fe-S] cluster in a similar position as the second cluster in the structure of biotin synthase (BioB) (*46*). The cluster is a [2Fe-2S] cluster separate from the radical SAM active site ligated by a separate set of cysteine amino acids. This indicates the possibility of a similar sulfur insertion mechanism as the other radical SAM enzymes BioB and lipoyl synthase (LipA). BioB's second cluster is a [2Fe-2S] cluster and provides one sulfur

atom derived from the cluster in the final step of biotin synthesis converting dethiobiotin to biotin (*80*). LipA contains a second [4Fe-4S] cluster and inserts two sulfurs in the transformation of octanoic acid to lipoic acid, with the second cluster of LipA suggested as the sulfur source (*81*, *82*). Therefore, it is possible that HydE utilizes its accessory Fe-S cluster as a source of sulfide in the synthesis of the bridging dithiolate ligand.

The aim of this project was to biochemically characterize active, Fe-S reconstituted HydE and to identify the substrate of this radical SAM enzyme. Accomplishing this provided a critical missing piece to H-cluster structure and biosynthesis, thereby helping to develop a fully *in vitro* activation of hydrogenase, which can be used in biotechnical applications for H_2 production, while at the same time providing possible clues to the origins of chemical complexity during the transition period from an abiotic to a biotic world. Moreover, characterization of HydE and its substrate molecule and chemical reaction will add fundamental new insights to the field of complex metallocofactor biosynthesis.

METHODS

Protein Expression and Purification

HydE in the absence of HydF and HydG ($HydE^{\Delta FG}$), HydF in the absence of HydE and HydG ($HydF^{\Delta EG}$), HydF in the presence of HydE and absence of HydG ($HydF^{E\Delta G}$), HydF in the absence of HydE and presence of HydG ($HydF^{G\Delta E}$), and HydF in the presence of HydE and HydG ($HydF^{EG}$) were heterologously expressed in a BL21 (DE3) *Escherichia coli* cell line as described previously (*83*). Single colonies from these transformations were grown in phosphate buffered Luria Broth (LB) media pH 7.5 for 12-15 hours at 37°C and 225 rpm shaking. These cells were used to inoculate larger cultures of 50 mM phosphate buffered (pH 7.5) LB media with 5 g/L NaCl, 5 g/L glucose to a final concentration of 5 mL/L inoculant. The cultures were grown at 37°C and 225 rpm shaking until they reached an optical density (OD_{600}) of 0.5, at which point they were induced with 1 mM isopropyl thiogalactopyranoside (IPTG). OD_{600} was measured using a Thermo Scientific Evolution 60 bench top UV-VIS spectrophotometer. 0.75 g/L ferrous ammonium sulfate (FAS) was added at the time of induction. Cultures were grown for 2.5 hours after induction at 37°C and 225 rpm shaking and then equilibrated to room temperature before another addition of FAS and sparging with N_2 for 12-15 hours at 4°C. Cells were harvested by centrifugation and the cell pellets were frozen at -80°C until further use.

Cell lysis and purification of the proteins were accomplished anaerobically in a Coy anaerobic chamber (Coy Laboratories, Grass Lake, MI). Cell pellets were

suspended in lysis buffer containing 50 mM HEPES pH 7.4, 10 mM imidazole, 500 mM KCl, 5% glycerol, 20 mM $MgCl_2$, 1 mM PMSF, 1% Triton X-100, 0.07 mg DNAse and RNAse per gram cell, and 0.6 mg lysozyme per gram cell. Cells were stirred in lysis mixture then centrifuged for 30 min at 18000 rpm. The supernatant was loaded onto a 5 mL HisTrap Ni^{2+}-affinity column (GE Healthcare) that was pre-equilibrated with Buffer A (50 mM HEPES pH 7.4, 500 mM KCl, 5% glycerol, 10 mM imidazole). After loading the supernatant onto the column, the column was washed with 10 column volumes of buffer A. Protein elution was achieved using a step-wise gradient of increasing imidazole in buffer B (50 mM HEPES pH 7.4, 500 mM KCl, 5% glycerol, 500 mM imidazole) from 10% buffer B, then 20%, then 50%, then 100%, with 5 column volumes at each stage. Fractions of high purity protein were dialyzed against 50 mM HEPES pH 7.4, 500 mM KCl, and 5% glycerol. Samples were then flash frozen then stored at -80°C until further use.

Protein purity was determined by SDS-PAGE analysis. Protein concentrations were determined by the method developed by Bradford using bovine serum albumin as the standard (*84*). Iron content was determined using the method developed by Fish (*85*).

Protein Reconstitution

Purified $HydE^{\Delta FG}$ had an initial iron content that was too low to be detected, so to increase iron loading of the protein, purified samples were chemically reconstituted under anaerobic conditions in a Coy anaerobic chamber. Reconstitution was achieved by addition of 5 mM DTT and an ~6-fold excess of $FeCl_3$ and Na_2S. After addition of $FeCl_3$

and Na_2S, samples were incubated for 2-3 hours then centrifuged to remove unbound iron and finally run over a G-25 Sephadex column to remove adventitiously bound iron using 50 mM HEPES pH 7.4, 500 mM KCl, and 5% glycerol as an eluent. Reconstitution efficiency was determined by UV/Vis absorption data acquired using a Cary 6000i UV/Vis/near-IR spectrophotometer (Varian). Reduced samples were prepared by the addition of 1 mM sodium dithionite. UV/Vis spectra were collected at a data interval of 0.5 nm and a scan rate of 60 nm/min. Protein samples were then concentrated to different volumes and concentrations using Amicon spin concentrators or sponge well concentrators.

EPR Sample Preparation and Spectroscopic Analysis

Electron paramagnetic resonance (EPR) samples of reconstituted HydE (154 µM) with an iron number of 3.36 ± 0.06 were prepared for analysis of the iron sulfur cluster content in an anaerobic MBraun Box (<1 ppm O_2). Oxidized samples were prepared by addition of 5 mM potassium ferricyanide and were incubated for 20 minutes before flash freezing. Photoreduced samples were prepared by supplementing the protein with 50 mM Tris pH 7.4, 100 µM deazariboflavin, and 5 mM dithiothreitol (DTT). Samples were then placed in an ice water bath and illuminated with a 300 watt Xe light for one hour. To an additional photoreduced sample, 1 mM SAM was added in the absence of light, and both samples were flash frozen in liquid nitrogen. Samples were stored in liquid nitrogen until spectroscopic analysis.

Low temperature EPR analysis was performed using a Bruker EMX X-band spectrometer equipped with a liquid helium cryostat and Oxford Instrument temperature controller. Typical EPR parameters were: 9.37 GHz microwave frequency, 1.84 mW microwave power, 12 K sample temperature, 81.92 ms time constant, and 167.7 s time sweep. EPR data simulation was performed using the EasySpin software program. To study the temperature dependence of the iron sulfur cluster content, the EPR spectrum of the photoreduced sample with added SAM was studied from 12 K up to 60 K in 10 K increments. The saturation of the EPR signal of the same sample with microwave power ranging from 18 μW to 36 mW was studied at 12 K. The experimental data were then plotted by comparing the log(signal/square root power) vs. the power as described in reference (*86*).

HydE Activity Assays

Radical SAM enzymes commonly cleave SAM very slowly in the absence of substrate, and a noticeable stimulation in the rate of SAM cleavage is observed when substrates or substrate analogs are present (*53, 58-70*). This differential rate of cleavage was utilized to provide evidence that HydG uses tyrosine as a substrate (*21*). Accordingly, activity assays of HydE were performed by quantifying the amount of deoxyadenosine produced in the absence and presence of different putative substrate molecules (Scheme 2.1).

Assays were carried out in an MBraun anaerobic chamber ($\leq$ 1 ppm O_2) at 37°C using an IsoTemp block. Assays consisted of a mixture of 25 μM HydE, 1mM SAM,

2mM dithionite, 50 mM HEPES pH 7.4, 500 mM KCl, and 5% glycerol, and other various additions. Metabolite additions were present at 2 mM unless noted otherwise. Aliquots were taken at various time points and the reaction was quenched with 1 M HCl. Samples were then prepared for analysis using HPLC by boiling then centrifuging the samples twice at 13,000 rpm for 10 minutes each. Samples were injected onto a Phenomenex Curosil PFP 5 µm, 4.6 x 150 mm analytical column that was pre-equilibrated in 98% solution A (0.1% acetic acid in water) and 2% solution B (0.1% acetic acid in acetonitrile) at 1 ml/min. The mobile phase was run at 98% A/2% B isocratically for 7 minutes after sample injection. A linear gradient was then run to 40% A/60% B over the next 17 minutes, and then this gradient was held for 3 minutes before re-equilibration at 98% A/2% B. Runs were all 35 minutes long and the column was held at 25°C. Elution of sample components was monitored at 254 nm. The rate of growth of the dAdo peak was an indicator for change in HydE activity. An increase in the rate of SAM cleavage by an added metabolite implicates it as the substrate.

To separate assays that included GTP, GDP, and deoxyadenosine, an alternate column and method were used. Samples prepared the same as above were injected onto a Symmetry C18 5 µm, 4.6 x 150 mm analytical column that was pre-equilibrated in 0% solution A (1:1 methanol:isopropanol) and 100% solution B (10 mM tetrabutyl ammonium bromide buffered with sodium phosphate, pH 6.5). The initial flow was 1.2 mL/min, which was then increased to 1.3 mL/min after 1 min. At 8 minutes, flow was then decreased to 1.2 mL/min, and the gradient was increased to 1% A/99% B. This was held for one minute, when flow was decreased to 1.1 mL/min and the gradient increased

to 2% A/98% B. This gradient was held constant as the flow was increased to 1.2 mL/min over the next 6 minutes. The gradient was increased to 4% A/96% B from 15 to 17 minutes, then held there until 19 minutes. It was then increased to 5% A/95% B from 19 minutes to 21 minutes and then increased again to 7% A/93% B from 21 minutes to 23 minutes. From 23 minutes to 25 minutes the flow was increased to 1.3 mL/min, and the gradient was decreased to 4% A/96% B, and then decreased again to 2% A/98% B from 25 minutes to 27 minutes. From 27 minutes to 29 minutes the flow was decreased to 1.2 mL/min, and the gradient was decreased to 1% A/99% B. Finally, from 29 minutes to 31 minutes the flow was decreased to 1.0 mL/min, and the gradient was decreased to 0% A/100% B, and then the column was re-equilibrated for an additional 9 minutes.

Assays for stimulation of dAdo production by other radical SAM enzymes PFL-AE and HydG were done using the same conditions listed above.

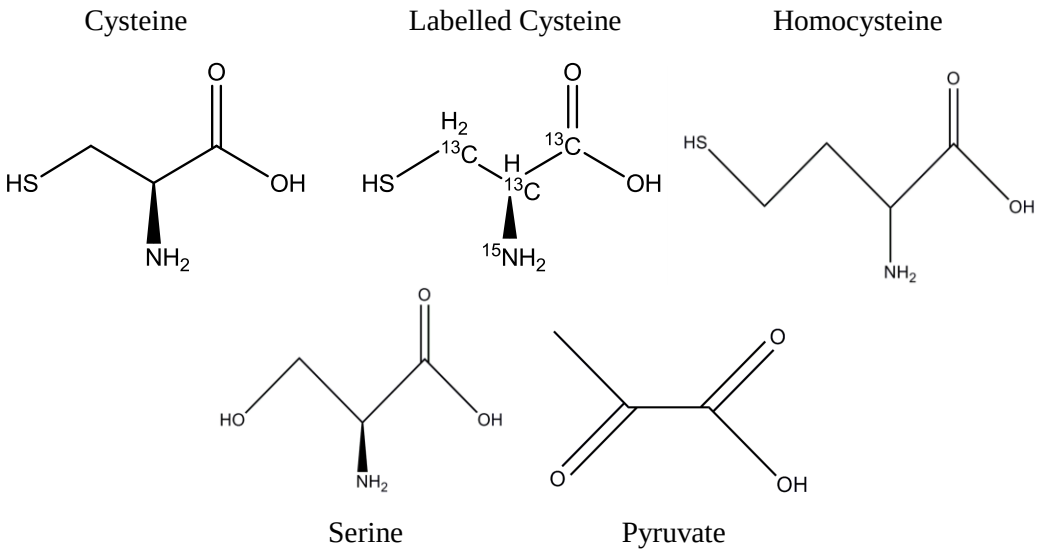

Scheme 2.1. Common metabolites of interest added to HydE activity assays.

Quantification of Glyoxylate by HPLC

The glyoxylate content of the samples was determined using a method as in reference (*87*). Glyoxylate was converted to the fluorescent 2-quinoxalinol using *o*-phenylene diamine (Scheme 2.2). 10 µL assay sample aliquots were diluted to 50 µL with 50 mM HEPES, pH 7.5, then 100 µL 0.5 M HCl and 50 µL of 10 mg/mL *o*-phenylene diamine dissolved in 0.5 M HCl. Samples were then incubated at 95°C for 10 min and then left at room temperature for 2 min before adding 120 µL 1.25 M NaOH. Samples were then flash frozen in liquid nitrogen before injection for LC-FLD. A calibration curve was prepared with the same method for final glyoxylate concentrations of 0, 3.5, 6.9, 13.9, 23.2, 37.1, and 55.7 µM.

The samples were injected onto a Phenomenex Hypersil BDS C_{18} 5µm, 4.6 x 150 mm column pre-equilibrated to 95% solvent A (100 mM ammonium bicarbonate) and 5% solvent B (100% acetonitrile). At 1 mL/min, 95% A/5% B was run for 5 min, followed by a gradient to 40% A/60% B over 15 minutes. The gradient was increased to 0% A/100% B over one min, which was held isocratically for 4 min. The gradient was then returned to 95% A/5% B over 0.5 min, and the column was re-equilibrated at this gradient for 10 min. The elution of 2-quinoxalinol was monitored using a fluorescence detector (λ_{ex} = 340 nm, λ_{em} = 420 nm).

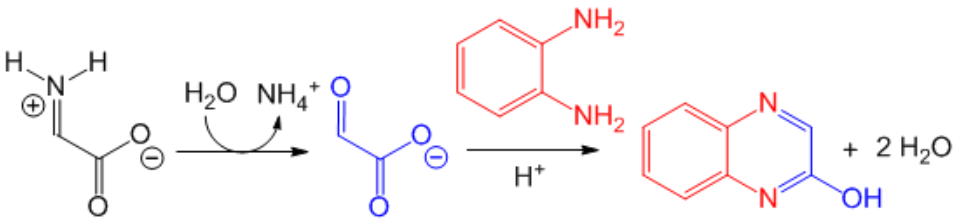

Scheme 2.2. Degradation of dehydroglycine to glyoxylate and derivitization of glyoxylate with *o*-phenylene diamine to form the fluorescent quinoxalinol. Reprinted from ref. 87.

Colorimetric Cysteine Assay

To determine the amount of cysteine left in a HydE activity assay after completion, a colorimetric cysteine assay derived from a method developed in reference (*88*) was used. Ninhydrin (Scheme 2.3) reacts with α-amino acids to form a purple color, and is a compound commonly used in finding fingerprints, but under normal conditions it does not react with the amino acids cysteine or proline. Under highly acidic and boiling conditions though, the reaction can be made highly specific for cysteine (*88*).

A ninhydrin stock was prepared by dissolving 250 mg in 6 mL of glacial acetic acid and 4 mL of concentrated HCl. The mixture requires ~20 min of constant mixing to dissolve. 25 µL of HydE activity samples were diluted to 500 µL with water. Then 500 µL of glacial acetic acid was added, and 500 µL of the ninhydrin stock was added after that. The samples were then boiled for 10 min before cooling them rapidly in an ice water bath and finally adding 8.5 mL of 95% ethanol. The absorbance of the samples was measured at 560 nm. A cysteine calibration curve was determined by diluting different amounts of a 5 mM stock to 500 µL and prepared as described above. The concentrations used for the standard curve were 0, 100, 200, 300, 400, and 500 µM

cysteine, as the concentration range for which the assay was linear was about half that reported in reference (*88*).

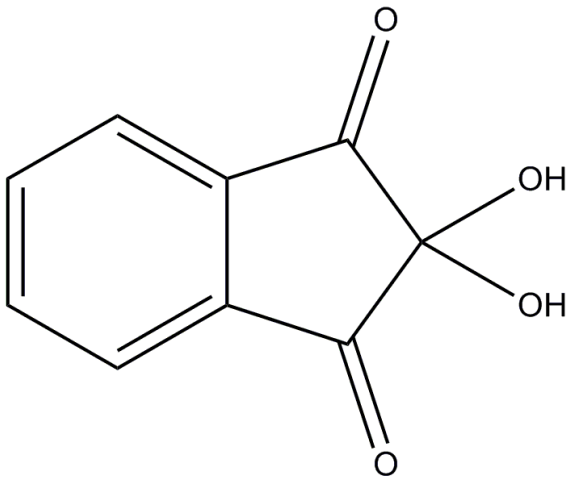

Scheme 2.3. Ninhydrin

RESULTS AND DISCUSSION

HydE Growth, Purification, and Characterization

Considerable progress in the purification and handling methods for $HydE^{\Delta FG}$ has been made. Despite many efforts, $HydE^{\Delta FG}$ still has inherent instability, providing low yields upon purification. A typical nine liter growth of *E. coli* designed to overexpress $HydE^{\Delta FG}$ yielded approximately 35 g of cells that were frozen and used for two purifications. One purification typically yielded approximately 10 mg of usable protein, giving an overall yield from one nine liter growth of about 20-25 mg usable $HydE^{\Delta FG}$. Purity of the protein was analyzed by SDS-PAGE. The peak fractions of the purified protein were light brown in color, and the color would be darker after dialysis and reconstitution, indicating the color originates from the Fe-S cluster content. Protein samples that were used in experiments were either non-concentrated samples at ~50 μM or samples concentrated to ~120 μM and contained 3.3 to 6.3 Fe atoms per protein. The large range of iron number in protein samples is likely due to the second [2Fe-2S] cluster not forming during chemical reconstitution in some samples.

Spectroscopic Characterization of HydE

UV-Visible spectroscopy of HydE shows spectra characteristic of [4Fe-4S] clusters. Figure 3.1 shows a spectrum of an as-isolated sample, reconstituted sample, and reduced reconstituted sample. The λ_{max} seen at 412 nm for the as isolated sample and 410 nm for the other two is characteristic of ligand to metal charge transfer between the sulfur

ligands and the Fe atoms of the [4Fe-4S] cluster. A slight shift and increase in intensity of λ_{max} from the as-isolated sample to the reconstituted is suggestive of successful incorporation of cluster content during reconstitution and is similar to successful reconstitutions previously seen with HydG (*73*). Fe content varies between reconstitution samples, and identified quantities have been in the range of 3.4 Fe/protein to 6.3 Fe/protein. Activity between samples was similar across the range of iron content.

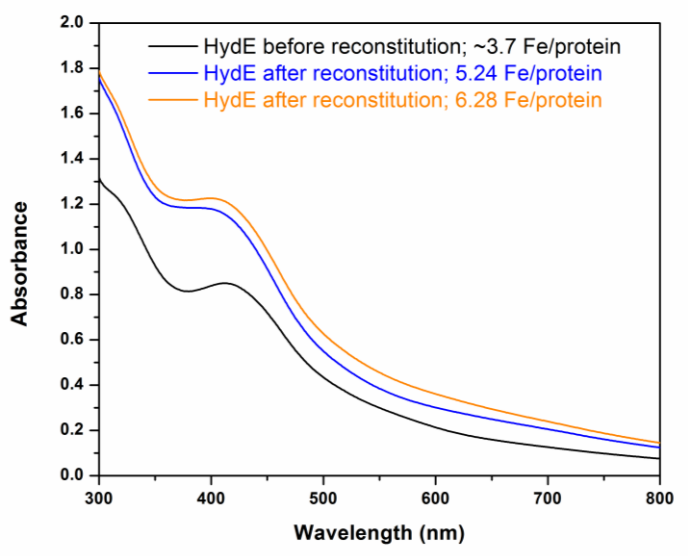

Figure 3.1. Representative UV-Vis spectrum of $HydE^{\Delta FG}$ [Fe-S] cluster reconstitution. Black represents unreconstituted sample, red and blue represent reconstituted sample. NBI-79: 82.87 µM, Fe content: ND; NBI-81 A: 49.12 µM, 5.24 Fe/mole of protein; NBI-81 B: 51.34 µM, 6.28 ± 0.095/mol of protein.

EPR spectroscopy has confirmed the presence of a [4Fe-4S] cluster and also indicates an interaction between the cluster and SAM. The as-isolated (reconstituted) enzyme (Fig. 3.2, green) showed a very small near isotropic signal indicative of a small percentage of clusters in a $[3Fe\text{-}4S]^{1+}$ state (0.02 spins/protein), with the majority likely being in the EPR silent $[4Fe\text{-}4S]^{2+}$ state. This near isotropic signal was greatly increased

in the oxidized enzyme (Fig 3.2, orange), indicating a larger percentage of the clusters being in the $[3Fe\text{-}4S]^{1+}$ state (0.13 spins/protein), which is common for site-differentiated clusters such as the one contained in radical SAM enzymes. The reduced enzyme (Fig 3.2, black) (0.37 spins/protein) exhibited a strong axial signal indicative of a $[4Fe\text{-}4S]^{1+}$ cluster. If one was to assume that all of the iron content of the protein was completely in the $[4Fe\text{-}4S]^{1+}$ state, it would correspond to 114 μM Fe spins in these samples. In the reduced signal, 0.37 spins/protein corresponds to 50.2 μM Fe spins, which represents 44% of that expected if the iron content is fully in the $[4Fe\text{-}4S]^{1+}$ state. The reason for the low number is that not all the Fe is in the $[4Fe\text{-}4S]^{1+}$ state; a very small amount is likely in a [2Fe-2S] cluster, and some is also likely adventitiously bound iron. Finally, the reduced enzyme in the presence of SAM (Fig 3.2, blue) (0.64 spins/protein) had an intense rhombic spectrum with the same oxidation state as the reduced cluster, but the binding of the SAM ligand to the site differentiated iron increases the distortion of the cluster. The spin quantification of this signal corresponds to 86.7 μM Fe spins, which is 76% of that expected if all the iron is in the $[4Fe\text{-}4S]^{1+}$ state. The reason for the greater number is that when SAM binds to the [4Fe-4S] cluster, it perturbs the redox potential of the cluster, which leads to greater reduction levels. The spin quantifications of the as-isolated sample and the oxidized sample correspond to very low iron spins because the majority of the Fe content in these samples is not in a paramagnetic state.

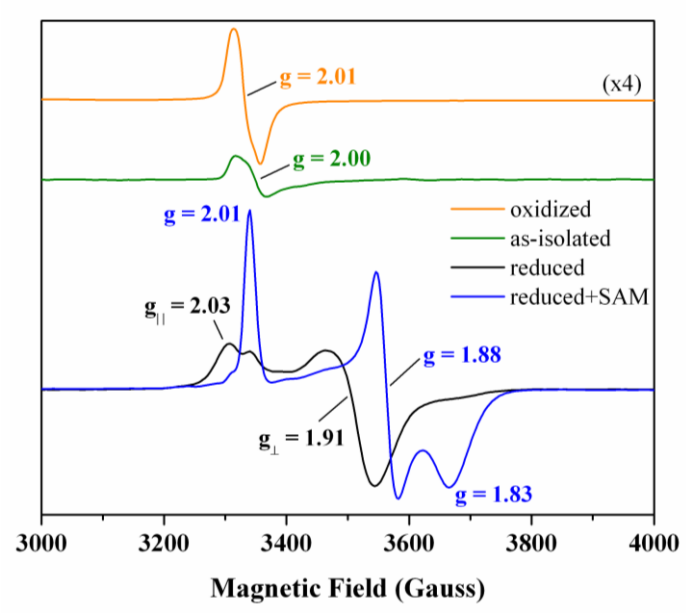

Figure 3.2. EPR Spectra of reconstituted HydE (154 µM, 3.37 ± 0.07 Fe/protein). Sample oxidized with 5mM ferricyanide and photoreduced in the presence and absence of 1 mM SAM. Samples were incubated 23 minutes prior to freezing, except for sample with SAM, which was incubated an additional 3 minutes. EPR parameters: 12 K, 9.37 GHz, 1.84 mW. EPR samples prepared and run by Dr. Eric Shepard.

The temperature dependence and power saturation of the reduced plus SAM sample were performed and further confirmed the cluster as a $[4Fe\text{-}4S]^{1+}$ cluster (Figure 3.3). As can be seen in panel A, by 30 K the rhombic signal had completely disappeared, and all that was left was a small nearly axial blip that remained all the way to 60 K. This rapid signal loss with increasing temperature is characteristic of a $[4Fe\text{-}4S]^{1+}$ cluster. The remaining signal at 60 K is suggestive of a $[2Fe\text{-}2S]^{1+}$ cluster with a signal relaxation that is much less dependent on temperature. This result is not unexpected, as there is a second cluster binding site in the protein, and the crystal structure previously solved from *Thermotoga maritima* contains a [2Fe-2S] cluster (*46*). The small signal at 60 K in Fig. 3.3 A indicates that the $[2Fe\text{-}2S]^{1+}$ content is minimal in this protein sample; the majority of cluster content in the sample is in the $[4Fe\text{-}4S]^{1+}$ state. The results shown in Fig 3.3

and 3.4 are from a protein sample containing 3.4 irons per protein, which qualitatively suggests that there is minimal [2Fe-2S] cluster content. This is consistent with results reported previously with a large range of iron content in reconstituted HydE (*65*) and that the second Fe-S cluster on HydE, the [2Fe-2S] cluster, never refines above 70% (*46*). The large disparity in iron content between protein preparations is likely due to the fact that the second cluster is fairly labile, as it only has three cysteine ligands with arginine acting as the fourth protein ligand to the cluster. Without EPR of the protein samples with greater iron content, it is not possible to determine whether that iron is truly part of a [2Fe-2S] cluster or if it is simply adventitiously bound iron, but it is important to note that during these studies, the SAM cleavage activity of the protein samples was unaffected by the differences in iron content. The power saturation (Fig. 3.3 B) is further confirmation of the fact that the primary cluster content is $[4Fe\text{-}4S]^{1+}$ since the log of the signal intensity over square root of power ($log\frac{S}{\sqrt{P}}$) versus power is roughly linear (*86*).

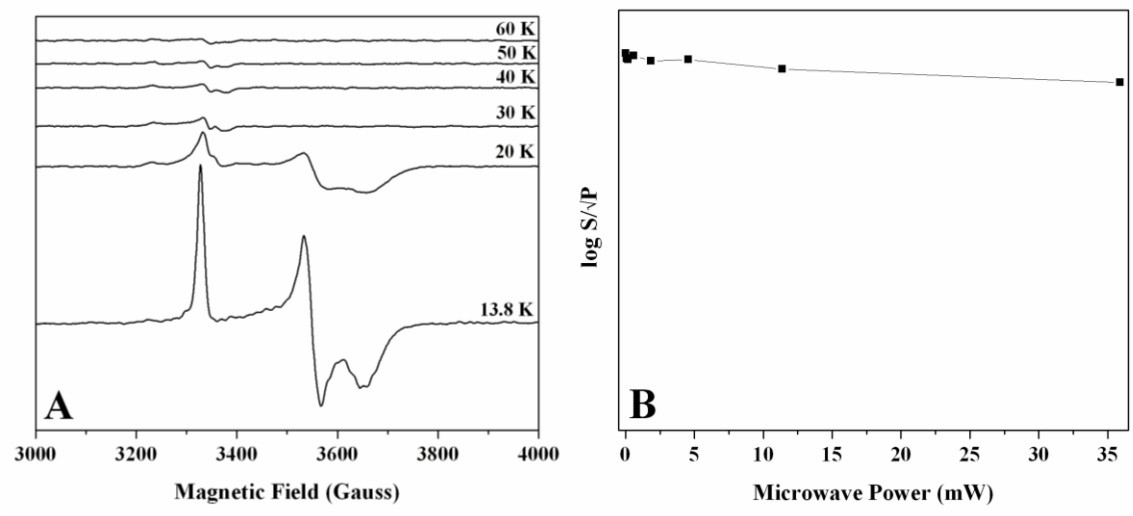

Figure 3.3. Temperature dependence (A) and power saturation (B) of the reduced + SAM HydE sample. Protein properties, sample preparation, and EPR parameters same as in Figure 3.3. EPR samples prepared and run by Dr. Eric Shepard.

Effect of Common Metabolites on HydE Activity

Activity assays of the HydE in these studies have shown that in the absence of any metabolite additions, HydE cleaves SAM and forms dAdo at a basal rate of 1 mol dAdo/mol HydE/hour, which is similar to that reported previously (*65*). Stimulation of this basal rate of SAM cleavage by the addition of a common metabolite could implicate it as the substrate.

A battery of common metabolites, including all amino acids except asparagine, were screened for their ability to stimulate the dAdo production of HydE. All but one of the amino acids tested, including homocysteine, resulted in no stimulation of HydE dAdo production (Fig. 3.4). Cysteine resulted in an approximately 50% increase in dAdo production by HydE. As seen in Figure 3.5, cysteine and serine were tested at multiple time points. Besides the 50% increase in dAdo production as measured at the 60 minute time point, the time-course study also shows that dAdo is formed at a faster rate than the basal rate of SAM cleavage. It can also be seen in this figure that serine, which is different from cysteine only by an oxygen atom in place of sulfur, has no effect on the formation of dAdo by HydE. This reproducible result suggests that cysteine is the substrate and that HydE is also dependent on the sulfur side group on cysteine instead of an oxygen side group on serine for stimulation of dAdo production.

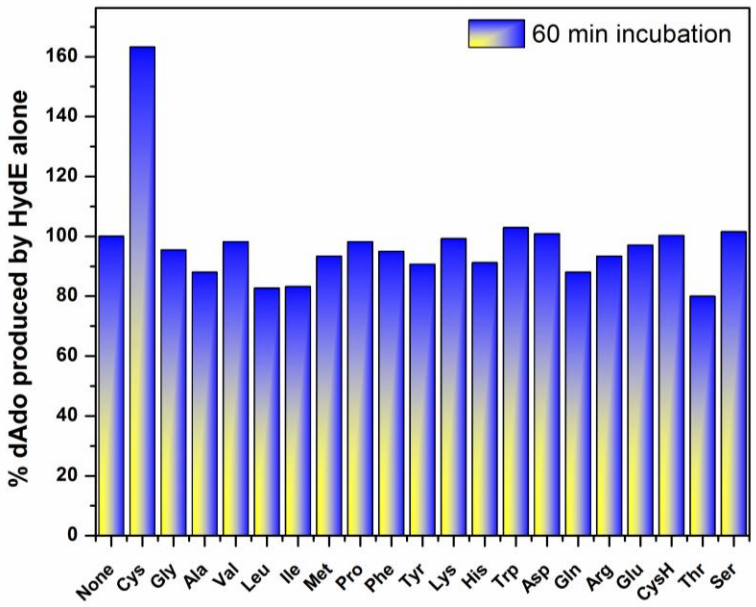

Figure 3.4. Effect of nineteen of twenty common amino acids and homocysteine on the activity of HydE as determined by dAdo production. Bars represent the percentage of dAdo produced by HydE with no additions after one hour.

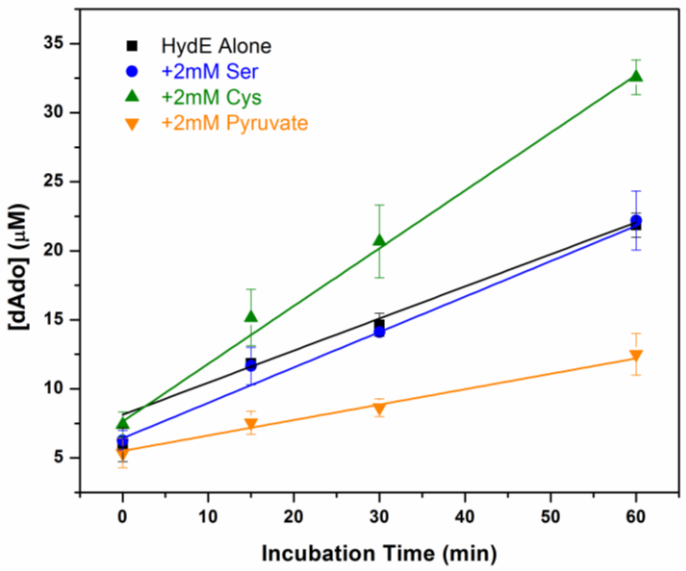

Figure 3.5. Effects of common metabolites on HydE activity. Assay consists of 25 μM HydE, 1mM SAM, 2 mM sodium dithionite, various metabolites at 2 mM, and 50 mM HEPES buffer to bring the assay up to volume. Error bars represent standard deviation of tests (n=3).

To insure that cysteine is not a general stimulant of radical SAM dAdo production, PFL-AE and HydG were tested to see if cysteine also enhanced the activity of these enzymes. Neither enzyme had increased activity as determined by dAdo production when cysteine was added to the assay mixture (data not shown).

From Figure 3.5, it can be seen that pyruvate inhibits the rate of dAdo formation by HydE. Two possibilities for this interesting result are that pyruvate could be a product analog and be providing product feedback inhibition on the enzyme, or it could be interacting with the site-differentiated iron on the radical SAM Fe-S cluster. Tests that could be done to analyze the cause for inhibition could be to see what type of inhibitor it is. Competitive inhibition could indicate pyruvate is interacting with SAM or the radical SAM cluster, while noncompetitive inhibition could possibly implicate pyruvate as a product analog. Another way to test whether pyruvate is interacting with SAM or the Fe-S cluster would be see whether pyruvate has a similar effect on other radical SAM enzymes.

Probing the Interaction between HydE and HydF$^{\Delta EG}$

Based on the current results of hydrogenase maturation, the current hypothesis is that HydE and HydG act on a pre-formed [2Fe-2S] cluster on HydF (*89*). If HydE is the source of the dithiolate ligand, one possibility is that it only needs to form the bridging ligand without sulfurs on the end, as the sulfur atoms in the final H-cluster may simply arise from the sulfides of the [2Fe-2S] cluster that acts as a scaffold for H-cluster assembly. This theory would suggest that HydF may be another ‘substrate’ of HydE or at

the very least interacts with HydE in some manner. An interaction between the two enzymes is also indicated by the fact that in eukaryotes, the HydE and HydF genes are fused. The crystal structure of HydE (*46*) shows a patch of ordered detergent molecules on a small part of the surface of the protein, indicating an area for interacting with another protein, either with another HydE to form a dimer or with one of the other Hyd maturase proteins.

Figure 3.6 panel A shows the effect of HydF in varying concentrations of the dAdo production of HydE. As the ratio of the concentration of HydF to HydE increases, the activity of HydE decreases, with a final decrease in activity of 39% when HydF is present at six times the amount of HydE. This result suggests that there is an interaction between the two enzymes, but the exact nature of the interaction is unclear at this point. As seen in Figure 3.6 panel B, even with cysteine present in the enzyme activity assay, HydF still has a slight inhibitory effect. The fact that HydF still inhibits HydE-catalyzed dAdo production with cysteine present suggests that the role of HydF is not to control the non-productive SAM cleavage by HydE, assuming that HydE is not non-productively cleaving SAM when cysteine is present.

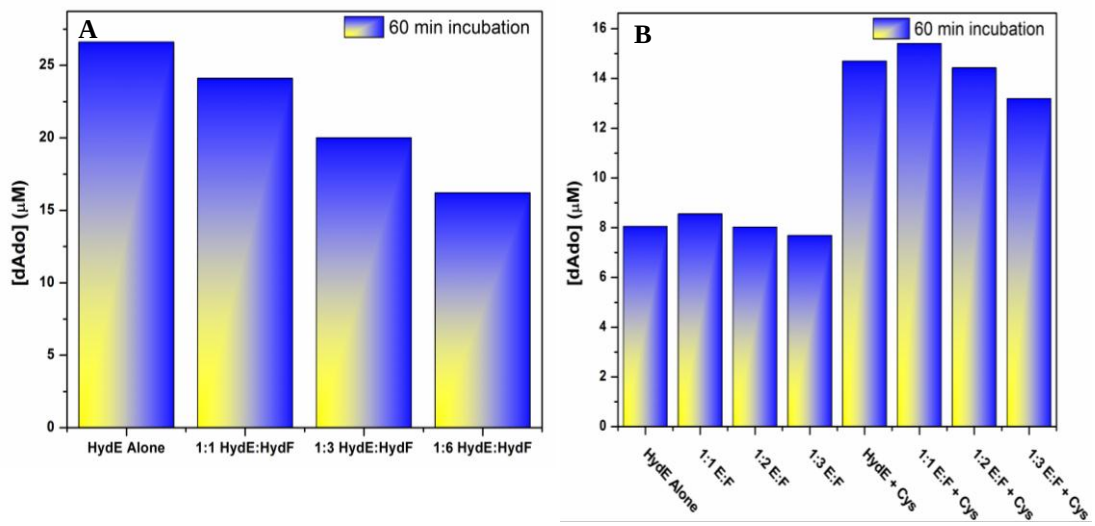

Figure 3.6. Effect of HydF on the activity of HydE. Assays performed the same as that described in figure 3.6, with increased concentrations of HydF in ratios described. (A) 60 minute incubation with broad range of ratios of HydE:HydF. (B) 60 minute incubation with and without cysteine.

Since the GTPase activity of HydF is increased by 50% when the radical SAM maturases HydE and HydG are present and because the GTPase activity of HydF has been shown to not be necessary for cluster transfer from HydF to [FeFe]-hydrogenase (*57*), it is possible that GTP hydrolysis by HydF is necessary for one of the radical SAM maturase activities. To test this possibility GTP and $MgCl_2$ were added to the HydE activity assays when HydF was also present. As can be seen in Figure 3.7, there is no effect of GTP on the activity of HydE when HydF is present. The reason for the very low activities shown in Figure 3.7 compared to the rest of the activities in this section is due to a different HPLC column used for analysis of these assays. The method and column used for all the other assays produced an exact overlap of the dAdo and GDP peaks on the HPLC chromatogram, making it difficult to quantify the dAdo produced. A modified program and column were used as described in the Methods, but the elution profile and

baseline for the molecules detected with this column was less than ideal, introducing a systematic amount of error in the integration of the dAdo (retention time (RT) = 19 min), GTP (RT = 24 min), and GDP (RT = 19.7 min) peaks. Despite the low values shown, it is still apparent that GTP has no effect on the activity of HydE. Since the alternate column has the ability to separate GTP and GDP these experiments also demonstrated that the HydF protein sample being used for these activity assays was an active sample, as the majority of the GTP in the samples was converted to GDP (data not shown).

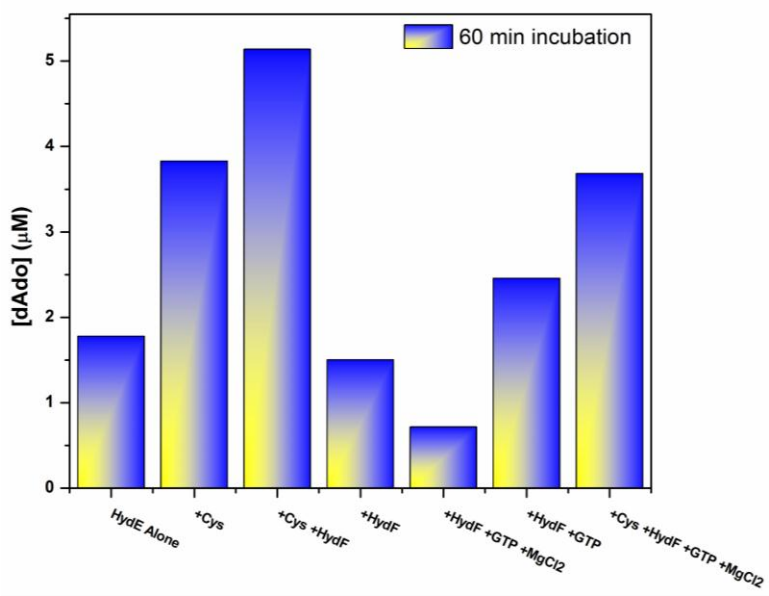

Figure 3.7. Effect of HydF on the activity of HydE when GTP is present. The HydE activity is lower in general for the whole experiment because the column used to separate GTP, GDP, SAM, and dAdo has a lower sensitivity for dAdo than does the one used in other experiments.

Exploring the Possibility of a Glyoxylate Intermediate

The enzymes HydG and a thiamine biosynthesis enzyme, ThiH, both utilize tyrosine as a substrate. It has been demonstrated that *p*-cresol and dehydroglycine are intermediates of the reaction of ThiH (*87*), and it has been suggested that HydG uses a

similar reaction mechanism with a dehydroglycine intermediate (*71*). Because HydG and HydE are both involved in H-cluster maturation and because they both recently diverged from a common chemical ancestor (*59*), it is also possible that they catalyze similar reactions, which could mean HydE also goes through a dehydroglycine intermediate. To test this hypothesis, assay products were derivatized to test for the presence of glyoxylate, the hydrolytic end-product of dehydroglycine.

Figure 3.8 shows the results of the glyoxylate concentration quantification. The first thing to note is that all of the concentrations are on the very low end of the detectable limit of the calibration curve, so although this method is very accurate, there may still be some error because of the low amounts present. Second, although there is a slight increase over time for each of the samples in glyoxylate concentration, it is important to note that there is a small amount of glyoxylate present in the samples where cysteine has not been added. Without cysteine in the assay, there should not be anything present that HydE could turnover to form glyoxylate. Additionally, when cysteine is added to the assays, the amount of glyoxylate produced should increase by a much larger amount than ~0.5 µM, which did not occur in this study. If the protein reaction product is not being disposed of, as it likely is during this *in vitro* study, it is possible that there will be a large amount of intermediates formed, which would hopefully be stoichiometric to the amount of dAdo produced in these assays. This condition would suggest that there should be up to 30 or 35 µM of glyoxylate formed over the course of an hour when cysteine is added to the assay, but again this is not seen. Given these results, it is unlikely that HydE acts on cysteine using the same mechanism as ThiH and the putative mechanism of HydG.

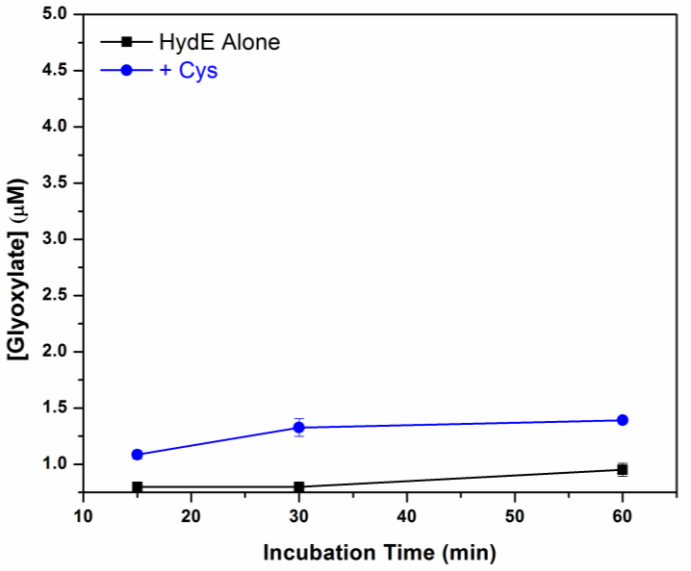

Figure 3.8. Glyoxylate quantification by HPLC. Glyoxylate concentration determined by conversion to the fluorescent 2-quinoxalinol using *o*-phenylene diamine. Error bars represent standard deviation of tests (n=2).

Testing for the Disappearance of Cysteine Over Time

Since methods exploring the end product of the HydE reaction, such as mass spectrometry, have proven difficult and have not yet yielded results, it is important to quantify the concentration of cysteine at any time during an activity assay. This was done using a colorimetric assay developed by M.K. Gaitonde in 1967 (*88*). Interestingly, Figure 3.9 shows that the cysteine concentration does not seem to be decreasing over time, but rather increasing over time. This highly reproducible result may indicate that a product of the HydE reaction is binding to the ninhydrin, since HydE cannot synthesize cysteine, or that cysteine disulfide present in the beginning of the reaction assay is being reduced to cysteine during the HydE reaction. Despite the fact that Gaitonde showed this assay is highly specific for cysteine (*88*), a second species that is similar enough to

cysteine that was not tested in the preliminary development of this assay may be binding to ninhydrin with a higher affinity and a higher extinction coefficient. An exploration into the reaction mechanism of formation of the ninhydrin complex could give insight into the identity of the second species binding to ninhydrin and potentially into the identity of the product of HydE. Mass spectrometry has again been difficult in trying to determine any identity because of the small masses of the molecules studied in this activity assay, as the differences in masses that need to be explored for this study are very small, and the masses of the species tested are on the lower end of the detectable limit. Additionally, most ionization methods for MS commonly completely fragment the small molecules or inconsistently couple them with other species in solution.

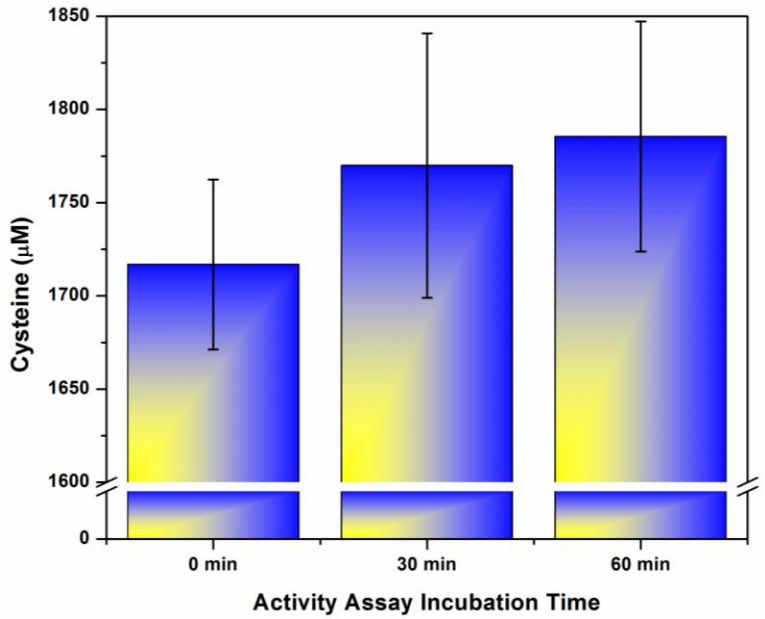

Figure 3.9. Colorimetric cysteine assay. Although it appears [cysteine] is increasing over time, some other species must be binding to ninhydrin with a greater extinction coefficient. Error bars represent standard deviation of tests (n=2).

Effect of Cysteine on HydF with Different Genetic Backgrounds

To test the effect cysteine has on the [2Fe-2S] cluster of HydF on systems with different genetic backgrounds (presence/absence of HydE/HydG), cysteine was added during cell growth for the $HydF^{EG}$, $HydF^{\Delta EG}$, $HydF^{E\Delta G}$ and $HydF^{G\Delta E}$ proteins. The proteins were then explored using visible spectroscopy. Figure 3.10 shows the UV-Vis spectra of the various proteins. In the proteins without cysteine added in the growth and $HydF^{\Delta EG}$ and $HydF^{G\Delta E}$ with cysteine added to the growth, there is a characteristic λ_{max} at 575 nm, which is the same as seen previously with $HydF^{\Delta EG}$ (*83*). In contrast $HydF^{E\Delta G}$ and $HydF^{EG}$ with cysteine added to the growth show a shift in the λ_{max} from 575 nm to 610 nm, again indicating that HydE is acting on cysteine to modify the [2Fe-2S] cluster of HydF. We propose that the 610 nm feature may represent an alkylated [2Fe-2S] cluster intermediate. The fact that cysteine only has an effect on the Fe-S cluster of HydF when HydE is in the genetic background is strong additional evidence that cysteine is the substrate of HydE and the source molecule for the bridging dithiolate ligand of the H-cluster of [Fe-Fe]-hydrogenase.

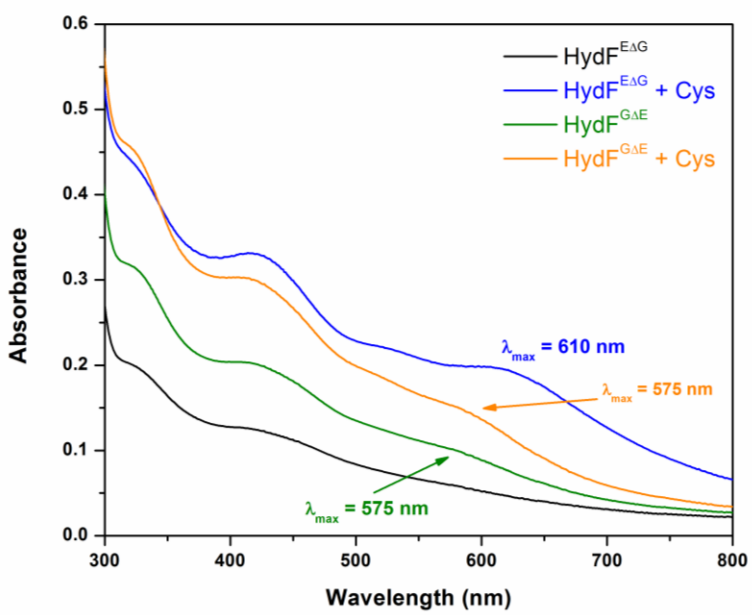

Figure 3.10. UV-Vis spectra of different HydF proteins. The λ_{max} is at 575 nm for all except HydF$^{E\Delta G}$ grown in presence of cysteine, which has a λ_{max} of 610 nm.

CONCLUSION AND FUTURE WORK

Biochemical characterization of HydE and identification of its substrate and product are crucial to a clearer understanding of H-cluster structure and maturation, which will be necessary before attempts to design biomimetic, hydrogen producing synthetic models as well as biotechnical applications. These synthetic constructs and biotechnical systems will hopefully decrease energy dependence on non-renewable resources and provide a better source for "clean" energy. Additionally, a better knowledge of H-cluster structure and maturation will provide insight into the origins of life and conditions and mechanisms of early life, since metal cofactor biosynthesis was likely one of the first steps between an abiotic and biotic world.

The data presented here offers compelling evidence that cysteine is the substrate of HydE. Stimulation of dAdo production by HydE is the most convincing evidence to implicate cysteine as the substrate. Additionally, the fact that of all the common metabolites and amino acids tested, including serine and homocysteine, which are very similar to cysteine, cysteine is the lone enhancer of SAM cleavage by HydE. At this point, it is not clear what the exact identity of the product of this reaction may be, but cysteine as a substrate makes sense for multiple reasons. First, cysteine is possibly one of the original amino acids, as it has a simple chemical make-up and sulfur was likely much more important and prominent in the time when life was just emerging (*90*). Second, because it is a small molecule to being with, this reaction likely provides a very chemically efficient way to produce the dithiolate ligand of the H-cluster, leaving little to waste. The simple molecule substrate and possible origins pre-dating the hydrogenase

system offer an additional argument for cysteine as the substrate. There are multiple possibilities for the reaction mechanism and product of the HydE cysteine reaction due to the unknown identity of the bridge head of the dithiolate ligand of the H-cluster. One potential mechanism would involve dehydration of the thiols of two cysteines followed by a condensation reaction to produce the bridge head, using the cysteine backbone for the other atoms of the dithiolate ligand. The second reaction would be slightly less favorable due to the large amount of substrate needed and chemical waste involved (R.Szilagyi, unpublished results).

Despite the questions that remain, much progress has been made with biochemically characterizing HydE and determining its substrate. Handling methods of the protein have been improved to give slightly better yields and better protein stability. It is clear that the substrate of HydE is cysteine and that the reaction of HydE with cysteine modifies the [2Fe-2S] cluster of HydF. The phenomenon is limited to when HydF is expressed in the background of HydE, indicating that it is not simply a general radical SAM function or hydrogenase maturation enzyme event when cysteine is present. The fact that cysteine consistently stimulates the SAM cleavage activity of HydE while no other small molecule tested does is the final piece of evidence to implicate cysteine as the small molecule substrate of HydE.

Future Work

There is much work that can still be done to elucidate the reaction mechanism and product of HydE. The first and most important task will be to continue improving

handling methods so that protein yields and stability can be increased. With greater protein stability and yields progress in biochemical characterization can be greatly accelerated, as the limiting factor for many experiments has been limited availability of usable protein. The next priority of HydE characterization is to discover the identity of the product of the HydE cysteine reaction. Using the same methods as described above for HydE activity assays to identify the product, mass spectrometry can be used to monitor the reaction, as a beginning (0 min) and end (60 min) time point could provide useful data as to what is produced and consumed during the reaction.

Once the product has been identified, it will be useful to get an X-ray crystal structure of HydE from *Clostridium acetobutylicum.* As shown above, a crystal structure has been solved for HydE, but it was for the enzyme from *Thermatoga maritima*, which has not yet been demonstrated to produce active HydA *in vitro*. Additionally, the structure solved previously was unable to provide any mechanistic insight since the study was unable to procure crystals with any potential substrates or products. Once the product has been identified using the methodology outlined above, the substrate and product (or potential analogs) can be soaked in crystals and structures obtained. These crystal soaking experiments would prove very useful in clarifying the reaction mechanism for HydE.

REFERENCES CITED

1. Beinert, H., Holm, R. H., and Munck, E. (1997) Iron-sulfur clusters: Nature's modular, multipurpose structures, *Science 277*, 653-659.

2. Beinert, H. (2000) Iron-sulfur proteins: ancient structures, still full of surprises (vol 5, pg 2, 2000), *Journal of Biological Inorganic Chemistry 5*, 409-409.

3. Jacobson, M. R., Cash, V. L., Weiss, M. C., Laird, N. F., Newton, W. E., and Dean, D. R. (1989) Biochemical and genetic analysis of the NifUSVWZM cluster from Azotobacter vinelandii, *Molecular & General Genetics 219*, 49-57.

4. Zheng, L. M., Cash, V. L., Flint, D. H., and Dean, D. R. (1998) Assembly of iron-sulfur clusters - Identification of an iscSUA-hscBA-fdx gene cluster from Azotobacter vinelandii, *Journal of Biological Chemistry 273*, 13264-13272.

5. Takahashi, Y., and Tokumoto, U. (2002) A third bacterial system for the assembly of iron-sulfur clusters with homologs in archaea and plastids, *Journal of Biological Chemistry 277*, 28380-28383.

6. Ayala-Castro, C., Saini, A., and Outten, F. W. (2008) Fe-s cluster assembly pathways in bacteria, *Microbiology and Molecular Biology Reviews 72*, 110-+.

7. Xu, X. M., and Moller, S. G. (2008) Iron-Sulfur Cluster Biogenesis Systems and their Crosstalk, *Chembiochem 9*, 2355-2362.

8. Kato, S., Mihara, H., Kurihara, T., Takahashi, Y., Tokumoto, U., Yoshimura, T., and Esaki, N. (2002) Cys-328 of IscS and Cys-63 of IscU are the sites of disulfide bridge formation in a covalently bound IscS/IscU complex: Implications for the mechanism of iron-sulfur cluster assembly, *Proceedings of the National Academy of Sciences of the United States of America 99*, 5948-5952.

9. Johnson, D. C., Unciuleac, M.-C., and Dean, D. R. (2006) Controlled expression and functional analysis of iron-sulfur cluster biosynthetic components within Azotobacter vinelandii, *Journal of Bacteriology 188*, 7551-7561.

10. Raulfs, E. C., O'Carroll, I. P., Dos Santos, P. C., Unciuleac, M.-C., and Dean, D. R. (2008) In vivo iron-sulfur cluster formation, *Proceedings of the National Academy of Sciences of the United States of America 105*, 8591-8596.

11. Mihara, H., and Esaki, N. (2002) Bacterial cysteine desulfurases: their function and mechanisms, *Applied Microbiology and Biotechnology 60*, 12-23.

12. Ding, H. G., and Clark, R. J. (2004) Characterization of iron binding in IscA, an ancient iron-sulphur cluster assembly protein, *Biochemical Journal 379*, 433-440.

13. Ding, H. G., Harrison, K., and Lu, J. X. (2005) Thioredoxin reductase system mediates iron binding in IscA and iron delivery for the iron-sulfur cluster assembly in IscU, *Journal of Biological Chemistry 280*, 30432-30437.

14. Yang, J., Bitoun, J. P., and Ding, H. (2006) Interplay of IscA and IscU in biogenesis of iron-sulfur clusters, *Journal of Biological Chemistry 281*, 27956-27963.

15. Lu, J., Yang, J., Tan, G., and Ding, H. (2008) Complementary roles of SufA and IscA in the biogenesis of iron-sulfur clusters in Escherichia coli, *Biochemical Journal 409*, 535-543.

16. Velayudhan, J., Castor, M., Richardson, A., Main-Hester, K. L., and Fang, F. C. (2007) The role of ferritins in the physiology of Salmonella enterica sv. Typhimurium: a unique role for ferritin B in iron-sulphur cluster repair and virulence, *Molecular Microbiology 63*, 1495-1507.

17. Bitoun, J. P., Wu, G., and Ding, H. (2008) Escherichia coli FtnA acts as an iron buffer for re-assembly of iron-sulfur clusters in response to hydrogen peroxide stress, *Biometals 21*, 693-703.

18. Expert, D., Boughammoura, A., and Franza, T. (2008) Siderophore-controlled Iron Assimilation in the Enterobacterium Erwinia chrysanthemi evidence for the involvement of bacterioferritin and the Suf iron-sulfur cluster assembly machinery, *Journal of Biological Chemistry 283*, 36564-36572.

19. Shima, S., Pilak, O., Vogt, S., Schick, M., Stagni, M. S., Meyer-Klaucke, W., Warkentin, E., Thauer, R. K., and Ermler, U. (2008) The crystal structure of Fe - hydrogenase reveals the geometry of the active site, *Science 321*, 572-575.

20. Volbeda, A., Charon, M. H., Piras, C., Hatchikian, E. C., Frey, M., and Fontecillacamps, J. C. (1995) Crystal structure of the Nickel-Iron hydrogenase from Desulfovibrio gigas, *Nature 373*, 580-587.

21. Reissmann, S., Hochleitner, E., Wang, H. F., Paschos, A., Lottspeich, F., Glass, R. S., and Bock, A. (2003) Taming of a poison: Biosynthesis of the NiFe-hydrogenase cyanide ligands, *Science 299*, 1067-1070.

22. Roseboom, W., Blokesch, M., Bock, A., and Albracht, S. P. J. (2005) The biosynthetic routes for carbon monoxide and cyanide in the Ni-Fe active site of hydrogenases are different, *Febs Letters 579*, 469-472.

23. McGlynn, S. E., Boyd, E. S., Shepard, E. M., Lange, R. K., Gerlach, R., Broderick, J. B., and Peters, J. W. (2010) Identification and Characterization of a Novel Member of the Radical AdoMet Enzyme Superfamily and Implications for the Biosynthesis of the Hmd Hydrogenase Active Site Cofactor, *Journal of Bacteriology 192*, 595-598.

24. Adams, M. W. W. (1990) The structure and mechanism of iron-hydrogenases, *Biochimica Et Biophysica Acta 1020*, 115-145.

25. Peters, J. W., Lanzilotta, W. N., Lemon, B. J., and Seefeldt, L. C. (1998) X-ray crystal structure of the Fe-only hydrogenase (Cpl) from Clostridium pasteurianum to 1.8 angstrom resolution, *Science 282*, 1853-1858.

26. Nicolet, Y., Piras, C., Legrand, P., Hatchikian, C. E., and Fontecilla-Camps, J. C. (1999) Desulfovibrio desulfuricans iron hydrogenase: the structure shows unusual coordination to an active site Fe binuclear center, *Structure with Folding & Design 7*, 13-23.

27. Peters, J. W. (1999) Structure and mechanism of iron-only hydrogenases, *Current Opinion in Structural Biology 9*, 670-676.

28. Nicolet, Y., Lemon, B. J., Fontecilla-Camps, J. C., and Peters, J. W. (2000) A novel FeS cluster in Fe-only hydrogenases, *Trends in Biochemical Sciences 25*, 138-143.

29. Lemon, B. J., and Peters, J. W. (1999) Binding of exogenously added carbon monoxide at the active site of the iron-only hydrogenase (CpI) from Clostridium pasteurianum, *Biochemistry 38*, 12969-12973.

30. Posewitz, M. C., King, P. W., Smolinski, S. L., Zhang, L. P., Seibert, M., and Ghirardi, M. L. (2004) Discovery of two novel radical S-adenosylmethionine proteins required for the assembly of an active Fe hydrogenase, *Journal of Biological Chemistry 279*, 25711-25720.

31. King, P. W., Posewitz, M. C., Ghirardi, M. L., and Seibert, M. (2006) Functional studies of FeFe hydrogenase maturation in an Escherichia coli biosynthetic system, *Journal of Bacteriology 188*, 2163-2172.

32. Mulder, D. W., Ortillo, D. O., Gardenghi, D. J., Naumov, A. V., Ruebush, S. S., Szilagyi, R. K., Huynh, B., Broderick, J. B., and Peters, J. W. (2009) Activation of HydA(Delta EFG) Requires a Preformed 4Fe-4S Cluster, *Biochemistry 48*, 6240-6248.

33. Frey, P. A., Hegeman, A. D., and Ruzicka, F. J. (2008) The radical SAM superfamily, *Critical Reviews in Biochemistry and Molecular Biology 43*, 63-88.

34. Shepard, E. M., and Broderick, J. B. (2010) S-Adenosylmethionine and Iron-Sulfur Clusters in Biological Radical Reactions: The Radical SAM Superfamily, In *Comprehensive Natural Products II* (Lew, M., and Hung-Wen, L., Eds.), pp 625-661, Elsevier, Oxford.

35. Krebs, C., Broderick, W. E., Henshaw, T. F., Broderick, J. B., and Huynh, B. H. (2002) Coordination of adenosylmethionine to a unique iron site of the 4Fe-4S of pyruvate formate-lyase activating enzyme: A Mossbauer spectroscopic study, *Journal of the American Chemical Society 124*, 912-913.

36. Walsby, C. J., Ortillo, D., Broderick, W. E., Broderick, J. B., and Hoffman, B. M. (2002) An anchoring role for FeS clusters: Chelation of the amino acid moiety of S-adenosylmethionine to the unique iron site of the 4Fe-4S cluster of pyruvate formate-lyase activating enzyme, *Journal of the American Chemical Society 124*, 11270-11271.

37. Walsby, C. J., Hong, W., Broderick, W. E., Cheek, J., Ortillo, D., Broderick, J. B., and Hoffman, B. M. (2002) Electron-nuclear double resonance spectroscopic evidence that S-adenosylmethionine binds in contact with the catalytically active 4Fe-4S (+) cluster of pyruvate formate-lyase activating enzyme, *Journal of the American Chemical Society 124*, 3143-3151.

38. Broderick, J. B., Walsby, C., Broderick, W. E., Krebs, C., Hong, W., Ortillo, D., Cheek, J., Huynh, B. H., and Hoffman, B. M. (2003) Paramagnetic resonance in mechanistic studies of Fe-S/radical enzymes, In *Paramagnetic Resonance of Metallobiomolecules* (Telser, J., Ed.), pp 113-127.

39. Walsby, C. J., Ortillo, D., Yang, J., Nnyepi, M. R., Broderick, W. E., Hoffman, B. M., and Broderick, J. B. (2005) Spectroscopic approaches to elucidating novel iron-sulfur chemistry in the "Radical-SAM" protein superfamily, *Inorganic Chemistry 44*, 727-741.

40. Lees, N. S., Chen, D., Walsby, C. J., Behshad, E., Frey, P. A., and Hoffman, B. M. (2006) How an enzyme tames reactive intermediates: Positioning of the active-site components of lysine 2,3-aminomutase during enzymatic turnover as determined by ENDOR spectroscopy, *Journal of the American Chemical Society 128*, 10145-10154.

41. Layer, G., Moser, J., Heinz, D. W., Jahn, D., and Schubert, W. D. (2003) Crystal structure of coproporphyrinogen III oxidase reveals cofactor geometry of Radical SAM enzymes, *Embo Journal 22*, 6214-6224.

42. Hanzelmann, P., and Schindelin, H. (2004) Crystal structure of the S-adenosylmethionine-dependent enzyme MoaA and its implications for molybdenum cofactor deficiency in humans, *Proceedings of the National Academy of Sciences of the United States of America 101*, 12870-12875.

43. Berkovitch, F., Nicolet, Y., Wan, J. T., Jarrett, J. T., and Drennan, C. L. (2004) Crystal structure of biotin synthase, an S-adenosylmethionine-dependent radical enzyme, *Science 303*, 76-79.

44. Lepore, B. W., Ruzicka, F. J., Frey, P. A., and Ringe, D. (2005) The x-ray crystal structure of lysine-2,3-aminomutase from Clostridium subterminale, *Proceedings of the National Academy of Sciences of the United States of America 102*, 13819-13824.

45. Goto-Ito, S., Ishii, R., Ito, T., Shibata, R., Fusatomi, E., Sekine, S.-i., Bessho, Y., and Yokoyama, S. (2007) Structure of an archaeal TYW1, the enzyme catalyzing the second step of wye-base biosynthesis, *Acta Crystallographica Section D-Biological Crystallography 63*, 1059-1068.

46. Nicolet, Y., Rubach, J. K., Posewitz, M. C., Amara, P., Mathevon, C., Atta, M., Fontecave, M., and Fontecilla-Camps, J. C. (2008) X-ray structure of the FeFe - hydrogenase maturase HydE from Thermotoga maritima, *Journal of Biological Chemistry 283*, 18861-18872.

47. Vey, J. L., Yang, J., Li, M., Broderick, W. E., Broderick, J. B., and Drennan, C. L. (2008) Structural basis for glycyl radical formation by pyruvate formate-lyase activating enzyme, *Proceedings of the National Academy of Sciences of the United States of America 105*, 16137-16141.

48. Chirpich, T. P., Zappia, V., Costilow, R. N., and Barker, H. A. (1970) Lysine 2,3-aminomutase- purification and properties of a pyridoxal phosphate and S-adenosylmethionine activated enzyme, *Journal of Biological Chemistry 245*, 1778-&.

49. Moss, M., and Frey, P. A. (1987) The role of S-adenosylmethionine in the lysine 2,3-aminomutase reaction, *Journal of Biological Chemistry 262*, 14859-14862.

50. Baraniak, J., Moss, M. L., and Frey, P. A. (1989) Lysine 2,3-aminomutase support for a mechanism of hydrogen transfer involving S-adenosylmethionine, *Journal of Biological Chemistry 264*, 1357-1360.

51. Yasbin, R. E., Cheo, D., and Bol, D. (1993) *DNA repair systems*.

52. Rebeil, R., Sun, Y. B., Chooback, L., Pedraza-Reyes, M., Kinsland, C., Begley, T. P., and Nicholson, W. L. (1998) Spore photoproduct lyase from Bacillus subtilis spores is a novel iron-sulfur DNA repair enzyme which shares features with proteins such as class III anaerobic ribonucleotide reductases and pyruvate-formate lyases, *Journal of Bacteriology 180*, 4879-4885.

53. Rebeil, R., and Nicholson, W. L. (2001) The subunit structure and catalytic mechanism of the Bacillus subtilis DNA repair enzyme spore photoproduct lyase, *Proceedings of the National Academy of Sciences of the United States of America 98*, 9038-9043.

54. Nicolet, Y., and Drennan, C. L. (2004) AdoMet radical proteins - from structure to evolution - alignment of divergent protein sequences reveals strong secondary structure element conservation, *Nucleic Acids Res. 32*, 4015-4025.

55. Curatti, L., Ludden, P. W., and Rubio, L. M. (2006) NifB-dependent in vitro synthesis of the iron-molybdenum cofactor of nitrogenase, *Proceedings of the National Academy of Sciences of the United States of America 103*, 5297-5301.

56. McGlynn, S. E., Mulder, D. W., Shepard, E. M., Broderick, J. B., and Peters, J. W. (2009) Hydrogenase cluster biosynthesis: organometallic chemistry nature's way, *Dalton Transactions*, 4274-4285.

57. Shepard, E. M., McGlynn, S. E., Bueling, A. L., Grady-Smith, C. S., George, S. J., Winslow, M. A., Cramer, S. P., Peters, J. W., and Broderick, J. B. (2010) Synthesis of the 2Fe subcluster of the FeFe -hydrogenase H cluster on the HydF scaffold, *Proceedings of the National Academy of Sciences of the United States of America 107*, 10448-10453.

58. Ollagnier, S., Mulliez, E., Schmidt, P. P., Eliasson, R., Gaillard, J., Deronzier, C., Bergman, T., Graslund, A., Reichard, P., and Fontecave, M. (1997) Activation of the anaerobic ribonucleotide reductase from Escherichia coli - The essential role of the iron-sulfur center for S-adenosylmethionine reduction, *Journal of Biological Chemistry 272*, 24216-24223.

59. Guianvarch, D., Florentin, D., Bui, B. T. S., Nunzi, F., and Marquet, A. (1997) Biotin synthase, a new member of the family of enzymes which uses S-adenosylmethionine as a source of deoxyadenosyl radical, *Biochemical and Biophysical Research Communications 236*, 402-406.

60. Shaw, N. M., Birch, O. M., Tinschert, A., Venetz, V., Dietrich, R., and Savoy, L. A. (1998) Biotin synthase from Escherichia coli: isolation of an enzyme-generated intermediate and stoichiometry of S-adenosylmethionine use, *Biochemical Journal 330*, 1079-1085.

61. Mulliez, E., Padovani, D., Atta, M., Alcouffe, C., and Fontecave, M. (2001) Activation of class III ribonucleotide reductase by flavodoxin: A protein radical-driven electron transfer to the iron-sulfur center, *Biochemistry 40*, 3730-3736.

62. Ollagnier-de Choudens, S., Sanakis, Y., Hewitson, K. S., Roach, P., Munck, E., and Fontecave, M. (2002) Reductive cleavage of S-adenosylmethionine by biotin synthase from Escherichia coli, *Journal of Biological Chemistry 277*, 13449-13454.

63. Zhao, X., Miller, J. R., Jiang, Y. F., Marletta, M. A., and Cronan, J. E. (2003) Assembly of the covalent linkage between lipoic acid and its cognate enzymes, *Chemistry & Biology 10*, 1293-1302.

64. Cicchillo, R. M., Iwig, D. F., Jones, A. D., Nesbitt, N. M., Baleanu-Gogonea, C., Souder, M. G., Tu, L., and Booker, S. J. (2004) Lipoyl synthase requires two equivalents of S-adenosyl-L-methionine to synthesize one equivalent of lipoic acid, *Biochemistry 43*, 6378-6386.

65. Rubach, J. K., Brazzolotto, X., Gaillard, J., and Fontecave, M. (2005) Biochemical characterization of the HydE and HydG iron-only hydrogenase maturation enzymes from Thermatoga maritima, *Febs Letters 579*, 5055-5060.

66. Layer, G., Grage, K., Teschner, T., Schunemann, V., Breckau, D., Masoumi, A., Jahn, M., Heathcote, P., Trautwein, A. X., and Jahn, D. (2005) Radical S-adenosylmethionine enzyme coproporphyrinogen III oxidase HemN - Functional features of the 4Fe-4S cluster and the two bound S-adenosyl-L-methionines, *Journal of Biological Chemistry 280*, 29038-29046.

67. Pieck, J. C., Hennecke, U., Pierik, A. J., Friedel, M. G., and Carell, T. (2006) Characterization of a new thermophilic spore photoproduct lyase from geobacillus stearothermophilus (SplG) with defined lesion containing DNA substrates, *Journal of Biological Chemistry 281*, 36317-36326.

68. Chandor-Proust, A., Berteau, O., Douki, T., Gasparutto, D., Ollagnier-de-Choudens, S., Fontecave, M., and Atta, M. (2008) DNA Repair and Free Radicals, New Insights into the Mechanism of Spore Photoproduct Lyase Revealed by Single Amino Acid Substitution, *Journal of Biological Chemistry 283*, 36361-36368.

69. Fontecave, M., Mulliez, E., and Logan, D. T. (2002) Deoxyribonucleotide synthesis in anaerobic microorganisms: The class III ribonucleotide reductase, *Progress in Nucleic Acid Research and Molecular Biology, Vol 72 72*, 95-127.

70. Pilet, E., Nicolet, Y., Mathevon, C., Douki, T., Fontecilla-Camps, J. C., and Fontecave, M. (2009) The role of the maturase HydG in FeFe -hydrogenase active site synthesis and assembly, *Febs Letters 583*, 506-511.

71. Nicolet, Y., Martin, L., Tron, C., and Fontecilla-Camps, J. C. (2010) A glycyl free radical as the precursor in the synthesis of carbon monoxide and cyanide by the FeFe -hydrogenase maturase HydG, *Febs Letters 584*, 4197-4202.

72. Driesener, R. C., Challand, M. R., McGlynn, S. E., Shepard, E. M., Boyd, E. S., Broderick, J. B., Peters, J. W., and Roach, P. L. (2010) FeFe -hydrogenase cyanide ligands derived from S-adenosylmethionine-dependent cleavage of tyrosine, *Angew Chem Int Ed Engl 49*, 1687-1690.

73. Shepard, E. M., Duffus, B. R., George, S. J., McGlynn, S. E., Challand, M. R., Swanson, K. D., Roach, P. L., Cramer, S. P., Peters, J. W., and Broderick, J. B. (2010) FeFe -Hydrogenase Maturation: HydG-Catalyzed Synthesis of Carbon Monoxide, *Journal of the American Chemical Society 132*, 9247-9249.

74. Silakov, A., Wenk, B., Reijerse, E., and Lubitz, W. (2009) N-14 HYSCORE investigation of the H-cluster of FeFe hydrogenase: evidence for a nitrogen in the dithiol bridge, *Physical Chemistry Chemical Physics 11*, 6592-6599.

75. Kuchenreuther, J. M., Stapleton, J. A., and Swartz, J. R. (2009) Tyrosine, Cysteine, and S-Adenosyl Methionine Stimulate In Vitro FeFe Hydrogenase Activation, *Plos One 4*.

76. Grigoropoulos, A., and Szilagyi, R. K. (2010) Evaluation of biosynthetic pathways for the unique dithiolate ligand of the FeFe hydrogenase H-cluster, *Journal of Biological Inorganic Chemistry 15*, 1177-1182.

77. Silakov, A., Reijerse, E. J., Albracht, S. P. J., Hatchikian, E. C., and Lubitz, W. (2007) The electronic structure of the H-cluster in the FeFe -hydrogenase from Desulfovibrio desulfuricans: A Q-band Fe-57-ENDOR and HYSCORE study, *Journal of the American Chemical Society 129*, 11447-11458.

78. Ryde, U., Greco, C., and De Gioia, L. (2010) Quantum Refinement of FeFe Hydrogenase Indicates a Dithiomethylamine Ligand, *Journal of the American Chemical Society 132*, 4512-+.

79. Nicolet, Y., Amara, P., Mouesca, J. M., and Fontecilla-Camps, J. C. (2009) Unexpected electron transfer mechanism upon AdoMet cleavage in radical SAM proteins, *Proceedings of the National Academy of Sciences of the United States of America 106*, 14867-14871.

80. Abdel-Hamid, A. M., and Cronan, J. E. (2007) In vivo resolution of conflicting in vitro results: Synthesis of biotin from dethiobiotin does not require pyridoxal phosphate, *Chemistry & Biology 14*, 1215-1220.

81. Miller, J. R., Busby, R. W., Jordan, S. W., Cheek, J., Henshaw, T. F., Ashley, G. W., Broderick, J. B., Cronan, J. E., and Marletta, M. A. (2000) Escherichia coli LipA is a lipoyl synthase: In vitro biosynthesis of lipoylated pyruvate dehydrogenase complex from octanoyl-acyl carrier protein, *Biochemistry 39*, 15166-15178.

82. Douglas, P., Kriek, M., Bryant, P., and Roach, P. L. (2006) Lipoyl synthase inserts sulfur atoms into an octanoyl substrate in a stepwise manner, *Angewandte Chemie-International Edition 45*, 5197-5199.

83. McGlynn, S. E., Shepard, E. M., Winslow, M. A., Naumov, A. V., Duschene, K. S., Posewitz, M. C., Broderick, W. E., Broderick, J. B., and Peters, J. W. (2008) HydF as a scaffold protein in FeFe hydrogenase H-cluster biosynthesis, *Febs Letters 582*, 2183-2187.

84. Bradford, M. M. (1976) Rapid and sensitive method for quantitation of microgram quantities of protein utilizing priniciple of protein-dye binding, *Analytical Biochemistry 72*, 248-254.

85. Fish, W. W. (1988) Rapid colorimetric micromethod for the quantitation of complexed iron in biological samples, *Methods in Enzymology 158*, 357-364.

86. Rupp, H., Cammack, R., Rao, K. K., and Hall, D. O. (1978) Electron-spin relaxation of iron-sulfur proteins studied by microwave-power saturation, *Biochimica Et Biophysica Acta 537*, 255-269.

87. Kriek, M., Martins, F., Challand, M. R., Croft, A., and Roach, P. L. (2007) Thiamine biosynthesis in Escherichia coli: Identification of the intermediate and by-product derived from tyrosine, *Angewandte Chemie-International Edition 46*, 9223-9226.

88. Gaitonde, M. K. (1967) A spectrophotometric method for direct determination of cysteine in presence of other naturally occurring amino acids, *Biochemical Journal 104*, 627-&.

89. Shepard, E. M., Boyd, E. S., Broderick, J. B., and Peters, J. W. (2011) Biosynthesis of complex iron-sulfur enzymes, *Current Opinion in Chemical Biology 15*, 319-327.

90. Parker, E. T., Cleaves, H. J., Dworkin, J. P., Glavin, D. P., Callahan, M., Aubrey, A., Lazcano, A., and Bada, J. L. (2011) Primordial synthesis of amines and amino acids in a 1958 Miller H2S-rich spark discharge experiment, *Proceedings of the National Academy of Sciences of the United States of America 108*, 5526-5531.